Photosynthesis Research (2020) 146:299–329
https://doi.org/10.1007/s11120-020-00777-0

ORIGINAL ARTICLE

Temperature-dependent regulation of electron transport and ATP synthesis in chloroplasts in vitro and in silico

Alexander N. Tikhonov[1,2] · Alexey V. Vershubskii[1]

Received: 15 April 2020 / Accepted: 21 July 2020 / Published online: 11 August 2020

Abstract

The significance of temperature-dependent regulation of photosynthetic apparatus (PSA) is determined by the fact that plant temperature changes with environmental temperature. In this work, we present a brief overview of temperature-dependent regulation of photosynthetic processes in class B chloroplasts (thylakoids) and analyze these processes using a computer model that takes into account the key stages of electron and proton transport coupled to ATP synthesis. The rate constants of partial reactions were parametrized on the basis of experimental temperature dependences of partial photosynthetic processes: (1) photosystem II (PSII) turnover and plastoquinone (PQ) reduction, (2) the plastoquinol (PQH_2) oxidation by the cytochrome (Cyt) b_6f complex, (3) the ATP synthase activity, and (4) the proton leak from the thylakoid lumen. We consider that PQH_2 oxidation is the rate-limiting step in the intersystem electron transport. The parametrization of the rate constants of these processes is based on earlier experimental data demonstrating strong correlations between the functional and structural properties of thylakoid membranes that were probed with the lipid-soluble spin labels embedded into the membranes. Within the framework of our model, we could adequately describe a number of experimental temperature dependences of photosynthetic reactions in thylakoids. Computer modeling of electron and proton transport coupled to ATP synthesis supports the notion that PQH_2 oxidation by the Cyt b_6f complex and proton pumping into the lumen are the basic temperature-dependent processes that determine the overall electron flux from PSII to molecular oxygen and the net ATP synthesis upon variations of temperature. The model describes two branches of the temperature dependence of the post-illumination reduction of P^+_{700} characterized by different activation energies (about 60 and ≤ 3.5 kJ mol^{-1}). The model predicts the bell-like temperature dependence of ATP formation, which arises from the balance of several factors: (1) the thermo-induced acceleration of electron transport through the Cyt b_6f complex, (2) deactivation of PSII photochemistry at sufficiently high temperatures, and (3) acceleration of the passive proton outflow from the thylakoid lumen bypassing the ATP synthase complex. The model describes the temperature dependence of experimentally measured parameter P/2e, determined as the ratio between the rates of ATP synthesis and pseudocyclic electron transport ($H_2O \rightarrow PSII \rightarrow PSI \rightarrow O_2$).

Keywords Photosynthesis · Chloroplasts · Electron transport · Thylakoid membranes · Temperature-dependent regulation · Computer modeling

Abbreviations

CBC	Calvin–Benson cycle
DGDG	Digalactosyldiacylglycerol
EPR	Electron paramagnetic resonance
ETC	Electron transport chain
Fd	Ferredoxin
FNR	Ferredoxin-NADP-oxidoreductase
ISP	Iron–sulfur protein
MGDG	Monogalactosyldiacylglycerol
ODE	Ordinary differential equations
Pc	Plastocyanin
PG	Phosphatidylglycerol
pmf	Proton-motive force
PSI and PSII	Photosystem I and photosystem II, respectively
PQ and PQH_2	Plastoquinone and plastoquinol (fully reduced form of PQ), respectively
P_{700}	Special chlorophyll pair in PSI, primary electron donor in PSI

✉ Alexander N. Tikhonov
an_tikhonov@mail.ru

[1] Faculty of Physics, M.V. Lomonosov Moscow State University, Moscow, Russia

[2] N.M. Emanuel Institute of Biochemical Physics of Russian Academy of Sciences, Moscow, Russia

P_{680}	Special chlorophyll pair in PSII, primary electron donor in PSII
Q_A and Q_B	Primary and secondary plastoquinone molecules bound to PSII
SQDG	Sulfoquinovosyldiacylglycerol
T	Temperature in Kelvin scale
t	Temperature in Celsius scale
τ	Time
WOC	Water-oxidizing complex
5-SASL	Spin probe 5-doxylstearate

Introduction

In plant cells, photosynthesis occurs in chloroplasts, the energy-transducing organelles that assimilate carbon dioxide (CO_2) and produce molecular oxygen (O_2) using the solar energy absorbed by photosynthetic antennas of photosystem I (PSI) and photosystem II (PSII). The protein–pigment complexes of PSI and PSII are embedded into the thylakoid membranes, which form closed vesicles surrounded by the chloroplast envelope. The piles of stacked flattened thylakoids form grana, which are linked to each other by means of the *inter*-granal thylakoids. The light energy absorbed by the light-harvesting complexes migrate to photoreaction centers of PSI and PSII (Nelson and Yocum 2006; Mamedov et al. 2015). Operating in tandem, PSI and PSII provide electron transfer from the water molecules, oxidized by the water-oxidizing complex (WOC) of PSII, to $NADP^+$, the terminal electron acceptor reduced by PSI. Two photosystems, PSII and PSI, are interconnected by the cytochrome (Cyt) b_6f complex and mobile electron carriers (plastoquinone and plastocyanin, PQ and Pc): PSII → PQ → Cyt b_6f → Pc → PSI → $NADP^+$. Photosynthetic electron transport is coupled to generation of the *trans*-thylakoid difference in electrochemical potentials of protons ($\Delta\tilde{\mu}_{H^+}$, termed as the proton-motive force, *pmf*), which is a source of energy to drive the H^+-ATP synthase: ADP + P_i → ATP (Boyer 1997; Walker 2013). NADPH and ATP, the macroergic products of the light-induced processes of photosynthesis, are used in biosynthetic reactions of the Calvin–Benson cycle (CBC) reactions (the fixation of CO_2 into carbohydrates) (Edwards and Walker 1983).

Photosynthetic protein complexes are embedded into the thylakoid membrane. Thylakoids are densely packed with proteins that constitute about 70% of membranes. The physico-chemical properties of the membrane bilayer are determined by the composition and characteristics of the individual lipids. There are four major glycerolipids of chloroplasts membranes: monogalactosyldiacylglycerol (MGDG), digalactosyldiacylglycerol (DGDG), sulfoquinovosyldiacylglycerol (SQDG), and phosphatidylglycerol (PG). Glycerolipids contain two fatty acids linked to glycerol. MGDG and DGDG are the main building blocks of the thylakoid membrane, which provide the matrix for embedding the photosynthetic complexes into the membrane. The membrane lipids allow lateral diffusion of plastoquinone molecules in the thylakoid membrane. MGDG and SQDG have been found in the Cyt b_6f complexes from plants and *Chlamydomonas*; lipids are involved in maintaining dimeric structure of photosynthetic electron transport complexes (Boudiere et al. 2014; Cramer and Hasan 2016).

The electron transport and ATP synthase complexes are distributed non-uniformly over the membranes of granal and stromal thylakoids (Albertsson 2001; Staehelin 2003; Dekker and Boekema 2005). Stacked thylakoids of grana are enriched with PSII; most of PSI and ATP synthase complexes are localized in the unstacked domains of stroma-exposed thylakoids, grana margins, and grana end membranes. The Cyt b_6f complexes are spread uniformly along the thylakoid membranes (Anderson 1982). There are two diffusion-controlled stages of the long-range communication between PSII and PSI: (i) electron transport from PSII to the Cyt b_6f complex mediated by PQH_2 molecules diffusing in the thylakoid membrane, and (ii) electron transfer from the Cyt b_6f complex to PSI mediated by Pc diffusing within the thylakoid lumen. The rate of the intersystem electron transport is determined by PQ turnover as a shuttle connecting PSII and Cyt b_6f complexes (Witt 1979; Haehnel 1984; Cardona et al. 2012). The rate of PQ turnover is determined by (*i*) the reduction of the secondary quinone Q_B to Q_BH_2, (*ii*) the dissociation of Q_BH_2 from PSII into the bulk phase of the thylakoid membrane ($Q_BH_2 \rightarrow PQH_2$), (iii) PQH_2 diffusion towards the Cyt b_6f complex, and (*iv*) PQH_2 oxidation at the Q_o site of the Cyt b_6f complex. The light-induced reduction of Q_B and the appearance of PQH_2 in PSII ($t_{1/2} \approx 0.6$–0.8 ms) occur more rapidly than the oxidation of PQH_2 by the Cyt b_6f complex ($t_{1/2} \geq 5$–20 ms, at room temperatures).

Plastoquinone diffusion in the lipid moiety of the membrane is a central event for the electronic connection between PSII and the Cyt b_6f complex. Over a wide range of pH, ionic strength, and temperature, the light-induced reduction of PQ to PQH_2, its dissociation from PSII and PQH_2 diffusion towards the Cyt b_6f complex occur more rapidly than PQH_2 oxidation (see Tikhonov 2013, 2014 and references therein). The electron transfer from PSII to the Cyt b_6f complex may be retarded due to slow percolation of PQH_2 through the lipid domains of the membrane over-crowded with protein complexes (Kirchhoff 2008, 2014). There are experimental reasons to believe, however, that the lateral diffusion of PQH_2 within the membrane, as well as Pc movement in the lumen, should not limit the overall rate of electron transfer between PSII and PSI (Haehnel 1976; Tikhonov et al. 1984). Indeed, although significant amounts of PSI and PSII complexes are laterally segregated, most of them are in close contact with the Cyt b_6f complexes, which are

evenly distributed over the thylakoid membrane (Albertsson 2001). The distribution of Cyt b_6f complexes among PSII supercomplexes localized in granal membranes minimizes the average distance traversed by plastoquinone molecules, providing rapid exchange of PQ and PQH_2 between the Cyt b_6f and PSII complexes (Kirchhoff et al. 2000; Tremmel et al. 2003). Obstructed diffusion of Pc within the narrow lumen may restrict electron communication between the Cyt b_6f and PSI complexes (Kirchhoff et al. 2011). However, electron transfer from the Cyt b_6f complex to Pc, and further from Pc^- to P^+_{700}, occurs more rapidly ($t_{1/2}$ ~ 5–350 µs, and $t_{1/2}$ ~ 20–200 µs) as compared to PQ turnover ($t_{1/2} \geq$ 4–20 ms) (Haehnel 1984; Sigfridsson 1998). Thus, Pc^- diffusion within the lumen should not limit the rate of the intersystem electron transport.

The intersystem electron transport is governed by the light-induced changes in the lumen pH (pH_{in}). There are two main mechanisms of the feedback control of photosynthetic electron transport: (i) the deceleration of PQH_2 oxidation by the Cyt b_6f complex caused by the lumen acidification (Tikhonov 2014, 2018 and references therein), and (ii) the attenuation of PSII activity due to ΔpH-dependent enhancement of thermal dissipation of absorbed light energy in LHCII known as non-photochemical quenching (NPQ) of chlorophyll (Chl) *a* excitation (Li et al. 2009; Demmig-Adams et al. 2012; Horton 2012). Thus, the light-induced acidification of the lumen reduces the rate of the intersystem electron transfer from PSII to PSI. There is also the mechanism of "metabolic" control, which means that the rate of electron flow in chloroplasts correlates with the so-called "phosphate potential", $P = [ATP]/([ADP] \times [P_i])$, where [ATP], [ADP], and $[P_i]$ are the concentrations of ATP, ADP, and P_i (Foyer et al. 2012). Depending on the ADP/ATP ratio, the ATP synthase functions either in the ATP synthesis mode or in the ATPase mode (ATP hydrolysis). In the metabolic "state 4" (the state of "photosynthetic control", exhausted pools of ADP and/or P_i), when the overall proton flux through the CF_0–CF_1 complex and ATP production virtually tend to zero, the intersystem electron flow decelerates due to sufficiently strong acidification of the lumen ($pH_{in} < 6$). In the metabolic "state 3", the rate of the intersystem electron flow is high, because ATP synthesis is accompanied by stoichiometric drain of protons from the lumen to stroma, thus precluding too strong acidification of the lumen ($pH_{in} \approx$ 6–6.2; Tikhonov 2013).

Photosynthetic apparatus is sensitive to changes in plant environment, including variations of temperature. The significance of temperature-dependent regulation of photosynthetic apparatus is determined by the fact that plants are poikilothermic organisms, meaning that their own temperature varies with environmental temperature. Thylakoid lipids play an important role in adaptation of chloroplasts to temperature variations. Galactolipids MGDG and DGDG are involved in the maintenance of membrane fluidity of the thylakoid membranes; they contain high amounts of polyunsaturated fatty acids. Adaptation of photosynthetic apparatus to low (or high) temperatures can proceed due to an increase (or a decrease) in the desaturation degree of fatty acids in galactolipids (Wallis and Browse 2002; Zhou et al. 2016). The response of photosynthetic apparatus to variations of temperature reveals itself as an interplay of a number of different partial photosynthetic processes. In the literature one can find varied information on temperature dependence of partial energy-transducing reactions in chloroplasts such as electron transfer and proton translocation (Kraayenhof et al. 1971; Shneyour et al. 1973; Nolan and Smillie 1976, 1977; Nolan 1980, 1981; Schuurmans and Kraayenhof 1983) and structural transitions in thylakoid membranes detected by the fluorescent and/or paramagnetic probes (Torres-Pereira et al. 1974; Yamamoto and Nishimura 1976; Murata and Fork 1977; Ford et al. 1982; Tikhonov and Subczynski 2005). It is remarkable that most of the Arrhenius plots for partial reactions of photosynthesis show inflexions (or even discontinuities) (Kumamoto et al. 1971; Inout 1978). There are, however, some inconsistent results on the estimation of the apparent activation energies formally determined for partial reactions near the transition temperatures. This diversity may be accounted for by using of various plant species and different experimental conditions.

Thermo-induced structural changes in thylakoid membranes belong to basic factors that determine the chloroplast response to fluctuations of temperature (for references, see Hirano et al. 1981; Barber et al. 1984; Los and Murata 2004; Tikhonov and Subczynski 2005; Allakhverdiev et al. 2008; Los et al. 2013; Yamori et al. 2014; Yamamoto 2016; Maksimov et al. 2017; Nievola et al. 2017; Hu et al. 2020). One of the mechanisms for supporting a sufficiently high activity of photosynthetic apparatus upon variations of temperature is associated with the reorganization of membrane structures, including changes in the physical state (fluidity) of the thylakoid membrane (Quinn and Williams 1978; Yamamoto et al. 1981; Mizusawa and Wada 2012; Yamori et al. 2014; Niu and Xiang 2018). Temperature-induced re-modeling of photosynthetic lipid–protein structures can affect the rates of electron and proton transport processes coupled to ATP synthesis, thereby providing optimal fitting of photosynthetic apparatus to environmental temperature. There are good reasons to believe that the acclimation of plants to environmental temperature is realized by changes in the composition of membrane lipids (saturated/desaturated lipids) that determine the local viscosity of the lipid domains (Heise and Harnischfeger 1978; Kern et al. 2009; Tietz et al. 2015; Maksimov et al. 2017). The fluidity of membrane lipids plays an important role in controlling photosynthetic processes. Variations of temperature directly alter the physical state of thylakoid membranes. Changes in the composition

of lipids (in particular, the relative content of unsaturated fatty acids) manifest themselves in temperature dependences of physical parameters of biological and model membranes (for references, see Berliner 1976; Griffith and Jost 1976; McConnell 1976; Lee 1977; Margolis et al. 1980; Luzikov et al. 1983, 1984; Aloia and Boggs 1985; Lutova and Tikhonov 1988). Lipids with unsaturated fatty acids have lower "melting" temperature than lipids containing saturated fatty acids; the proportionality between these lipids is one of the key factors that determine the membrane fluidity and lipid diffusion in the thylakoid membranes (Sarcina et al. 2003; Tietz et al. 2015). A decrease in the fluidity of lipid domains of thylakoid membranes caused, for example, by the implementation of cholesterol, is accompanied by an inhibition of the intersystem electron transfer (Yamamoto et al. 1981; Ford and Barber 1983; Barber et al. 1984). The ratio of saturated and unsaturated fatty acids depends on the plant growth conditions (Sawada and Miyachi 1974). Fluidity of membrane lipids is often considered as a peculiar sensor that triggers the retrograde signals controlling the expression of desaturases, adjusting the thylakoid membrane to environmental temperature and, thereby, optimizing the energy transduction in photosynthetic organisms (Los and Murata 2004; Los et al. 2013).

In our previous works (Tikhonov et al. 1980, 1981, 1983, 1984; Timoshin et al. 1984; Tikhonov and Subczynski 2005), we used the electron paramagnetic resonance (EPR) technique for scrutinizing the structure–function relationships in class B chloroplasts (thylakoids) isolated from bean leaves. The advantage of the EPR method is that it allows measuring the functional (electron transport) and structural characteristics of thylakoid membranes under the same experimental conditions. Class B chloroplasts present a suitable model for analyzing the regulation of photosynthetic processes, because they are deprived of the outer shell and the CBC enzymes. This is because the processes beyond the thylakoids will not interfere with the membrane-dependent reactions of electron transport. In the meantime, the integrity of closed thylakoids enables them to generate $\Delta\tilde{\mu}_{H^+}$ and to support the operation of the ATP synthase. Investigating the structure–function relationships in bean thylakoids, we have found strong correlations between the temperature dependences of the intersystem electron transport and ATP synthesis, on the one hand, and structural changes in the lipid domains of thylakoid membranes, on the other hand (the results of these studies are briefly summarized in Tikhonov and Subczynski (2005) and Tikhonov (2020)). The lipid-soluble nitroxide radicals (spin probes) were used for probing the structural transitions in the lipid domains of thylakoid membranes. These changes manifest themselves as the inflexions (or breaks) in the plots of spectral parameters. The EPR spectra of spin probes depend on their local surroundings and ordering of nitroxide radicals in the membrane moiety. It is important to note, however, that spin probes localized at different depths from the membrane surface indicate on the cooperative character of *thermo*-induced structural transients in the lipid domains of thylakoid membranes (Lee 1977; Tikhonov and Subczynski 2005).

The current work was inspired by the necessity of numerical simulation of temperature-dependent photosynthetic processes in chloroplasts. The importance of computer modeling of temperature-dependent photosynthetic processes is determined by the complexity and variability of electron and proton transport events in chloroplasts (for reviews, see Kukushkin and Tikhonov 1988; Karavaev and Kukushkin 1993; Laisk et al. 2009; Lazár and Schansker 2009; Riznichenko et al. 2009; Arnold and Nikoloski 2011; Igamberdiev 2011; Zaks et al. 2012; Zhu et al. 2013; Rubin and Riznichenko 2014; Tikhonov and Vershubskii 2014; Tikhonov 2016; Stirbet and Govindjee 2016; Cherepanov et al. 2017; Morales et al. 2018; Stirbet et al. 2014, 2019). The responses of photosynthetic apparatus to temperature manifest itself as the interplay of different processes; temperature-dependent regulation of photosynthesis is achieved by cooperation of several feedbacks. Computer modeling of photosynthetic processes would gain a better insight into understanding the temperature-dependent regulation of photosynthesis, which is important from both fundamental and applied viewpoints. The main purpose of this study is the computer analysis of relationships between electron transport, proton translocation, and ATP synthesis processes in thylakoids. Our model mimics the influence of the membrane physical state on the key steps of electron transport in thylakoids. Below, describing the model, we briefly overview the relationships between the photosynthetic processes (electron transport, proton translocation, and ATP synthesis) and structural transitions in the lipid domains of bean thylakoids. Results of our calculations strongly support the notion that the structural changes in the lipid domains and protein complexes, which control the photochemical activity of PSII, the rate of PQH_2 oxidation by the Cyt b_6f complex and the *trans*-thylakoid proton transfer through the ATP synthase, are among the crucial factors of the temperature-dependent regulation of electron transport and ATP synthesis in chloroplasts.

Description of the model

General properties of the model

Figure 1 (the bottom panel a) depicts the layout of electron carriers functioning in the chain of electron transport from H_2O to O_2 through the membrane-bound protein complexes (PSII, b_6f, and PSI) and mobile electron carriers, plastoquinone (PQ). The model describes the

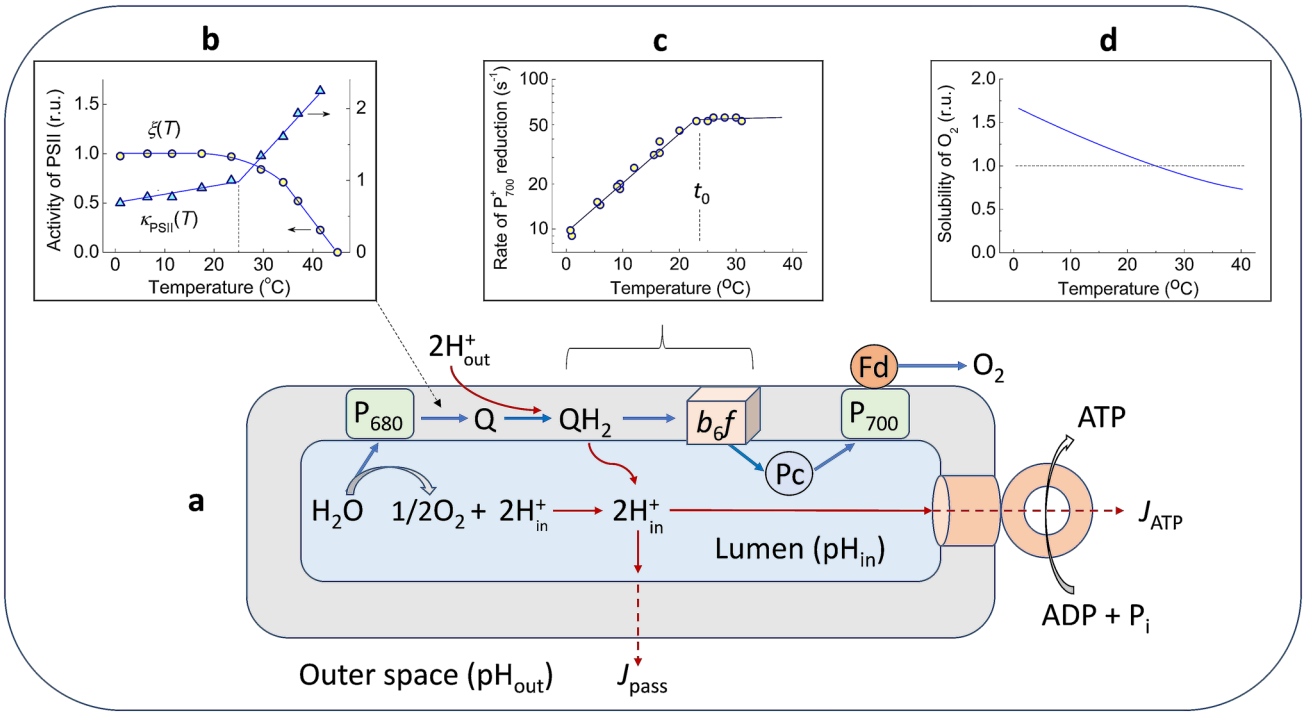

Fig. 1 A scheme of the photosynthetic electron and proton transport processes considered in the model and the arrangement of the four main protein complexes (photosystem I, photosystem II, cytochrome b_6f, and ATP synthase) in the thylakoid membrane (panel **a**). Blue arrows show electron transfer reactions, and red arrows depict proton transport pathways. The top panels **b**, **c**, and **d** illustrate the impact of temperature on the partial reactions in the chain of linear electron transport. Panel **b** shows the temperature dependences of the model parameters $\xi(T)$ and $\kappa_{PSII}(T) = f(T)/f_o$, which determine the operation of PSII (based on data presented in Tikhonov et al. 1983; see text for explanations). Parameter $\xi(T)$ characterizes the photochemical activity of PSII in response to a short light flash (7 μs) inducing single turnover of PSII. Parameter $\kappa_{PSII}(T)$ characterizes acceleration of electron transfer from P680 to the PQ pool (for details, see text and Fig. 13 in "Appendix 3"). Panel **c** shows the temperature dependence of parameter $\tau_{1/2}^{-1}$, where $\tau_{1/2}$ is the half-time of the post-illumination reduction of P_{700}^+ (based on data presented in Tikhonov et al. 1984). Panel **d** shows the temperature dependence of O_2 solubility in water solutions (based on data presented in Melnichenko et al. 2008)

key stages of electron transfer from the water-oxidizing complex (WOC) of PSII to molecular oxygen, the terminal electron acceptors of PSI in class B chloroplasts ($H_2O \rightarrow PSII \rightarrow PQ \rightarrow b_6f \rightarrow Pc \rightarrow PSI \rightarrow O_2$). Mobile electron carriers, plastoquinone (PQ) and plastocyanin (Pc), mediate electron transfer between the PSII, Cyt b_6f, and PSI complexes. Reduced plastoquinol molecules (PQH_2) connect PSII with the Cyt b_6f complex. PQH_2 oxidation by the Cyt b_6f complex is considered as the rate-limiting step in the intersystem chain of electron transport. We take into account that the rate of PQH_2 oxidation is controlled by the *intra*-thylakoid pH (pH_{in}), because the PQH_2 oxidation is coupled to dissociation of two protons into the thylakoid lumen ($PQH_2 \rightarrow PQ + 2H_{in}^+ + 2e^-$). Pc molecules, reduced by the Cyt b_6f complexes, rapidly moving within the lumen, provide the reduction of P_{700}^+. As noted above, the PQH_2 formation in PSII and its diffusion to the Cyt b_6f complex usually occur more rapidly ($\tau_{1/2}$ < 1–5 ms) than electron transfer from PQH_2 to P_{700}^+ ($\tau_{1/2}$ > 5–20 ms) via the Cyt b_6f complex and Pc (for references, see Siggel 1976; Sanderson et al. 1986; Sigfridsson 1998; Hope 2000; Santabarbara et al. 2009; Tikhonov 2013, 2014, 2018). This means that the rate of P_{700}^+ reduction by electrons injected to the intersystem ETC from PSII should be determined predominantly by the rate of electron transfer from the PQH_2 pool to the Cyt b_6f complex. On the acceptor side of PSI, reduced ferredoxin molecules bound to PSI (F_A and/or F_B) donate electrons to O_2. Molecular oxygen which serves as the terminal electron acceptor in the chain of pseudocyclic ETC (the "water-water" cycle; Asada 1999; Ort and Baker 2002; Cherepanov et al. 2017), since type B chloroplasts have no envelope, and thus neither FNR nor the CBC enzymes.

Electron transport processes are accompanied by translocation of protons into the thylakoid lumen ($H_{out}^+ \rightarrow H_{in}^+$) and generation of the *trans*-thylakoid pH difference ($\Delta pH = pH_{out} - pH_{in}$). The acidification of the lumen ($pH_{in} < pH_{out}$) occurs due to functioning of WOC in PSII and the PQ shuttle ($PQ + 2e^- + 2H_{out}^+ \rightarrow PQH_2 \rightarrow PQ + 2e^- + 2H_{in}^+$). The proton leakage from the lumen occurs by two ways: (a) the proton flux through the ATP synthase (J_{ATP}),

coupled to ATP formation from ADP and inorganic phosphate P_i, and (b) the passive proton flux through the membrane (J_{pass}). We assume that the pH value of the suspension is constant ($pH_{out} = 8$), owing to sufficiently high buffer capacity of the external medium.

The following variables of the model are considered: the relative concentrations of oxidized primary electron donors in PSI and PSII ($[P^+_{700}]$ and $[P^+_{680}]$); the relative concentration of oxidized plastoquinone, [PQ]; the relative concentration of oxidized ferredoxin bound to PSI, [Fd]; the relative concentration of oxidized plastocyanin, [Pc]. The proton transport is described by the variable $[H^+_{in}]$, the concentration of hydrogen ions within the lumen. The light-induced changes in ATP concentration, described by the variable [ATP], is determined by the balance between the ATP synthesis and the ATP hydrolysis processes as described earlier (Tikhonov and Vershubskii 2014; Vershubskii et al. 2017). The model parameters L_1 and L_2 characterize the photosynthetically active fluxes of light quanta exciting PSI and PSII, respectively. The ratio $L_1/L_2 = 10$ was accepted for mimicking the far-red light ("Light 1") exciting preferentially PSI. The ratio $L_1/L_2 = 1$ was used for modeling illumination of chloroplasts by light efficiently exciting both PSI and PSII ("Light 2").

A system of non-linear ordinary differential equations (ODE) was used to describe the dynamics of the model system (for details, see Tikhonov and Vershubskii 2014; Vershubskii et al. 2017, 2018). The set of ODE is presented in "Appendix 1". The appropriate choice of the apparent rate constants of partial reactions of electron and proton transport was described in our previous works (Vershubskii et al. 2011; see also Table 1 in "Appendix 1"). We have analyzed chloroplast functioning in three metabolic states: state 3 refers to the quasi-steady-state of chloroplasts during active ATP synthesis in the presence of the surplus amounts of ADP and P_i, state 4 corresponds to the state of "photosynthetic control" (no total synthesis of ATP), state 5 pertains to the situation when $\Delta pH = 0$ (uncoupled thylakoids).

Effects of temperature on the partial reactions of electron transport in thylakoids

The top panels in Fig. 1 illustrate how variations of temperature influence the photochemical activity of PSII (panel **b**), the rate of electron transfer from PQH_2 to P^+_{700} (via the Cyt b_6f complex and Pc; panel **c**), and the solubility of O_2 in water solutions (panel **d**). We analyze electron transport processes in the temperatures range from 0 to 45 °C, because the PSII activity is known to be completely inhibited at temperatures ≥ 45 °C (see, e.g., Lutova and Tikhonov 1983; Benkov et al. 2019). Parametrization of temperature dependences of the partial reactions of electron transport is based on experimental data borrowed from our previous works on class B bean chloroplasts (Tikhonov et al. 1980, 1983, 1984; Timoshin et al. 1984). Below we briefly consider the peculiarities of temperature-dependent partial reactions of electron and proton transport considered in this work. Plant materials and some principal details of experimental methods used in the above-cited works are presented in "Appendix 3".

Photosystem II

For parametrization of PSII activity, we used the temperature dependences of the relative numbers of electrons injected into the intersystem ETC in response to light flashes of various duration (Tikhonov et al. 1980; Tikhonov and Vershubskii 2017; for details, see "Appendix 3"). The model parameters $\xi(T)$ and $\kappa_{PSII}(T)$ characterize the temperature dependence of PSII activity. Parametrization of $\xi(T)$ was performed on the basis of the kinetics of P_{700} redox transients induced by a short pulse ($t_{1/2} = 7$ µs) of white light of saturating intensity, which provided a single turnover of PSII (Stiehl and Witt 1969; Witt 1979). Parameter $\xi(T)$ decreases at temperatures ≥ 25 °C (Fig. 1b), tending to zero at 45 °C (complete inhibition of PSII activity).

In response to a long flash ($t_{1/2} = 750$ µs), each PSII donated several electrons to the PQ pool. We assume that the apparent rate constant of electron transfer from PSII to PQ (the rate constant $k_{P_{680}}$, Eq. A4 in "Appendix 1") to be proportional to the ratio $f = W_2(T)/W_1(T)$, where $W_2(T)$ and $W_1(T)$ denote the relative numbers of electrons donated into the intersystem ETC in response to the long ($\tau_{1/2} = 750$ µs) and short ($\tau_{1/2} = 7$ µs) flashes, respectively (for definition of W_2 and W_1, see Fig. 13 in "Appendix 3"). Figure 1b shows the temperature dependence of the ratio $f(T) = W_2/W_1$ normalized to $f_0 = f(25\ °C)$. Parameter $\kappa_{PSII}(T) = f(T)/f\ (25\ °C)$ increases with the rise of temperature. This means that the apparent rate constant of electron transfer from PSII to the PQ pool increases with temperature. A clear inflexion of $\kappa_{PSII}(T)$ at 25 °C is likely to reflect structural changes in the membrane that have impact on PSII activity. In order to simulate the influence of the membrane physical state on the rate of electron transfer from PSII to the PQ pool, we performed calculations for different patterns of $\kappa_{PSII}(T)$, characterized by different values of the model parameter t_o (Fig. 2a).

PQH_2 oxidation

Modeling the chain of linear electron transfer ($H_2O \rightarrow$ PSII $\rightarrow$ PQ $\rightarrow b_6f \rightarrow$ Pc $\rightarrow$ PSI $\rightarrow$ Fd $\rightarrow O_2$), we assume that the reaction of PQH_2 oxidation is the rate-limiting step in the intersystem ETC (Stiehl and Witt 1969). In the whole range of temperatures considered in our work (0–45 °C), the rate of PQH_2 oxidation is significantly slower than the Pc turnover between the Cyt b_6f complex and PSI (see, e.g., Tikhonov et al. 1984, 2018 and references therein). Rapid

shuttling of electrons between the PSII and Cyt b_6f complexes is determined by a high mobility of PQH_2 and PQ molecules of the photo-reducible plastoquinone pool in the thylakoid membrane. Close location of PSII and granal Cyt b_6f complexes and sufficiently high fluidity of membrane lipids promote rapid formation of the "substrate–enzyme" complex (PQH_2-b_6f). The overall rate of the intersystem electron transfer should be determined mainly by the rate of PQH_2 oxidation at the quinol-binding portal Q_o of the Cyt b_6f complex (Tikhonov 2014, 2016, 2018). The rate of this process is controlled by the intra-thylakoid pH (pH_{in}). Oxidation of PQH_2 is accompanied by the release of two protons into the lumen. The back-pressure of the protons pumped into the lumen decelerates the oxidation of PQH_2, thereby slowing down the intersystem electron transport with the lumen acidification ($pH_{in}\downarrow$).

Within the framework of our model, we consider the influence of pH_{in} on the rate of PQH_2 oxidation, using the function $k_Q^0\left([PQ],[Pc],[H_{in}^+]\right) = 1/\tau_Q$, which was first suggested by Dubinskii and Tikhonov (1997). We used this function in our works (Vershubskii et al. 2011, 2018; Tikhonov and Vershubskii 2014, 2017), assuming that the rate of PQH_2 oxidation can be found as the reciprocal value of the overall time τ_Q of PQH_2 turnover related to electron flow from PQH_2 to Pc via the Cyt b_6f complex:

$$\tau_Q = \frac{1}{k_o \cdot [PQH_2]} + \tau_1^o \cdot \left(1 + [H_{in}^+]/h_1\right) + \tau_2^o \cdot \left(1 + [H_{in}^+]/h_2\right) + \frac{1}{2k_f \cdot [Pc]}. \quad (1)$$

The τ_Q value is the sum of characteristic times related to the following steps of PQH_2 oxidation by the Cyt b_6f complex and further electron transfer to Pc: (1) the PQH_2 binding to quinol-binding center "o", (2) the two-electron oxidation of PQH_2, and (3) the electron transfer from the Cyt b_6f complex to plastocyanin (Pc). Here, $[PQH_2] = [PQ]_0 - [PQ]$ is the concentration of PQH_2, k_o is the binding constant of PQH_2 to the Q_o center; τ_1^o,τ_2^o, h_1, and h_2 are the model parameters characterizing two steps of PQH_2 oxidation inside the Cyt b_6f complex; k_f is the rate constant of electron transfer from the Cyt b_6f complex to the oxidized Pc molecule. Parameters h_1 and h_2 are the normalizing coefficients, the magnitudes of which are determined by the pK_a values of the first and second stages of PQH_2 deprotonation. The deprotonation of PQH_2, associated with the proton release into the lumen, to be considered as the prerequisite for PQH_2 oxidation (Brandt 1996; Link 1997; Crofts et al. 2000, 2013). Therefore, the rate of PQH_2 oxidation appears to be dependent on the concentration of hydrogen ions ($[H_{in}^+]$) inside the thylakoids (for references, see Tikhonov 2013, 2014, 2018). In this work, the choice of the coefficients related to parametrization of $k_Q^0\left([PQ],[Pc],[H_{in}^+]\right)$ was performed as described earlier (Vershubskii et al. 2011, 2018; Tikhonov and Vershubskii 2014; see also "Appendix 1"). A good agreement between the experimental and model pH_{in} dependences of the kinetic parameter $\tau_{1/2}$, which characterizes the half-time of the post-illumination reduction of P_{700}^+, proves an adequacy of $k_Q^0\left([PQ],[Pc],[H_{in}^+]\right)$ parametrization (see Fig. 13 in "Appendix 3").

The oxidation/reduction reactions of plastoquinone are the temperature-dependent processes. In the current work, we used the modified function $k_Q^0\left([PQ],[Pc],[H_{in}^+]\right)$ to describe the temperature dependence of the intersystem electron transfer. According to experimental data for bean chloroplasts (for review, see Tikhonov 2018, 2020 and reference therein), the temperature dependence of the rate of electron transfer from PQH_2 to P_{700}^+ can be approximated by two exponents (Fig. 1c). Taking that at the characteristic temperature t_0 the rate of PQH_2 oxidation can be described by the function $k_Q^0\left([PQ],[Pc],[H_{in}^+]\right)$, we determined the function $k_Q\left([PQ],[Pc],[H_{in}^+],T\right)$ using the following formula:

$$k_Q\left([PQ],[Pc],[H_{in}^+],T\right) = \kappa_Q(T)k_Q^0\left([PQ],[Pc],[H_{in}^+]\right), \quad (2)$$

where $\kappa_Q(T) = \exp\left[-E_a/\left(k_B T\right) + E_a/\left(k_B T_0\right)\right]$ is the temperature-dependent correction factor. Here, E_a is the activation energy, k_B is the Boltzmann constant, T denotes the temperature in the Kelvin scale, $T_0 = 273.16 + t_0$, where t_0 is the peculiar temperature in the Celsius scale. The function $k_Q^0\left([PQ],[Pc],[H_{in}^+]\right)$ describes the overall rate of PQ turnover at the characteristic temperature t_0, which corresponds to the break-point in the temperature dependence of the PQH_2 oxidation rate determined from the post-illumination reduction of P_{700}^+. According to experimental data on bean chloroplasts presented in Tikhonov et al. (1984), the Arrhenius plot of the overall rate of electron transfer from PQH_2 to P_{700}^+ can be approximated by two exponents with activation energies $E_a^{(1)}$ and $E_a^{(2)}$. Experimental Arrhenius plot of the rate of the post-illumination reduction of P_{700}^+ (Fig. 1c) shows an explicit break at $t_0 \approx 25$ °C and characterized by $E_a^{(1)} \approx 60$ kJ/mol and $E_a^{(2)} \leq 3.5$ kJ/mol. There are good reasons to believe that the two branches in the temperature-dependence plot reflect structural transitions in the lipid domains of the thylakoid membrane. Thus, bearing in mind the structure–function relationships in thylakoid membranes, we can say that the two-branch pattern of the temperature-dependent correction factor $\kappa_Q(T)$, and, respectively, the function $k_Q\left([PQ],[Pc],[H_{in}^+],T\right)$, mimic the temperature dependence of PQH_2 oxidation at different fluidities of the membrane (see Tikhonov 2020 and references therein). In this work, we compared the behavior of the model system for three different patterns of the temperature-dependent correction factor $\kappa_Q(T)$ (Fig. 2b).

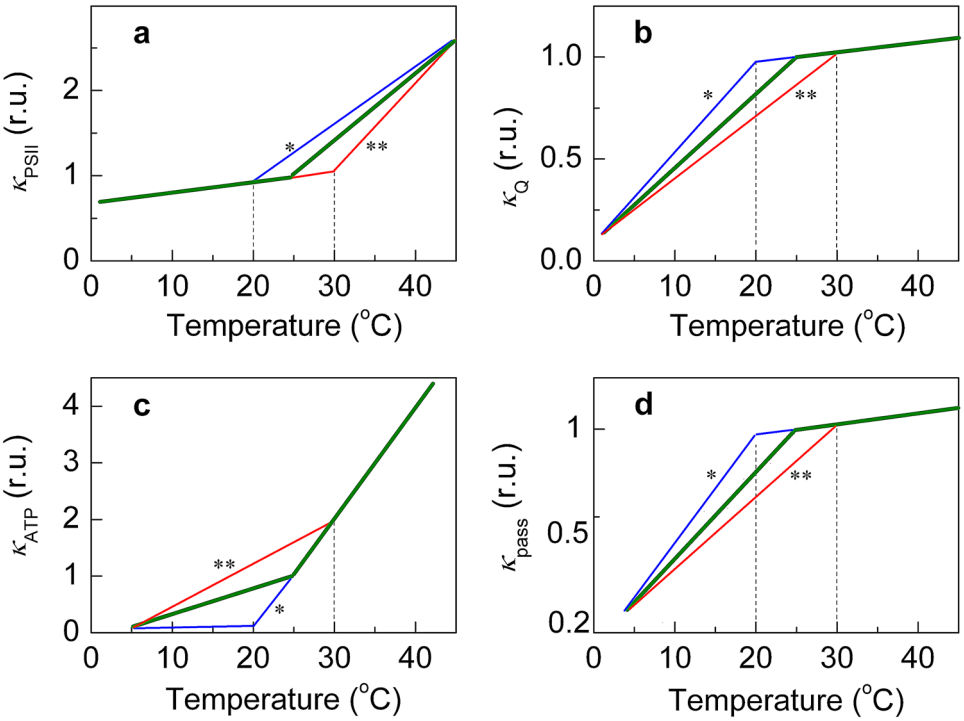

Fig. 2 Temperature dependences of the partial reactions of photosynthesis related to different values of the model parameters t_0. The value of parameters t_0 reflects the temperature of the membrane structural transition (for more explanations, see the main text): $t_0 = 20$ °C (labeled by one asterisk), $t_0 = 25$ °C (the basic model), and $t_0 = 30$ °C (labeled by two asterisks). Panel **a**: Normalized temperature dependence of the correction factor $\kappa_{PSII}(T) = f(T)/f(t_0)$, where the ratio $f(T) = W_2(T)/W_1(T)$ characterizes the acceleration of PSII turnover with temperature (for definition of $W_2(T)$ and $W_1(T)$, see Fig. 13 in "Appendix 3"). Panel **b**: Normalized temperature dependence of the correction factor $\kappa_Q(T)$ characterizing the rate of electron transfer from PQH_2 to Pc via the Cyt b_6f complex (see text for explanations). Panel **c**: Normalized temperature dependence of the correction factor $\kappa_{ATP}(T)$ characterizing the effect of temperature on the activity of the ATP synthase complex. Panel **d**: Normalized temperature dependence of the correction factor $\kappa_{pass}(T)$ characterizing the passive H^+ ion transfer through the thylakoid membrane

Photosystem I

Electron transfer on the acceptor side of PSI occurs rapidly by the mechanism of quantum mechanical tunneling (Moser et al. 1992; Brettel 1997; Page et al. 1999; Möbius and Savitsky 2009; Shelaev et al. 2010). The outflow of electrons from PSI to O_2 (the Mehler reaction; see Asada 1999; Badger et al. 2000; Ort and Baker 2002; Cherepanov et al. 2017) was calculated as $J_{Fd-O2} = k_{Meh}\cdot(1 - [Fd])\cdot[O_2]$. Here, k_{Meh} stands for the apparent rate constant of electron transfer from the reduced terminal electron carriers on the acceptor side of PSI (F_A and F_B), collectively denoted as Fd, and $[O_2]$ is the concentration of molecular oxygen in the chloroplast suspension. As a result of electron transfer from PSI to O_2, superoxide radicals $O_2^{\bullet-}$ are formed. Two $O_2^{\bullet-}$ molecules dismutate to form hydrogen peroxide (H_2O_2) and molecular oxygen O_2 ($2O_2^{\bullet-} + 2H^+ \rightarrow H_2O_2 + O_2$), and two H_2O_2 molecules decompose to O_2 and water. Thus, electrons from the water molecules oxidized in PSII are transferred to O_2 ($O_2 + e^- \rightarrow O_2^{\bullet-}$); the water molecule formed in the result of further transformations of $O_2^{\bullet-}$ is the final product of PSI ($H_2O \rightarrow$ PSII $\rightarrow$ PSI $\rightarrow H_2O$, the "water–water" cycle; Asada 1999).

It is common knowledge that PSI is less sensitive to injuries at higher temperatures compared to PSII. Variations of temperature within the range 0–45 °C may influence PSI activity, but much less significantly than the intersystem electron transport controlled by PQ reduction by PSII and PQH_2 oxidation by the Cyt b_6f (see, e.g., Yan et al. 2013). Nevertheless, the terminal stage of electron transfer (the reduction of O_2 by Fd^-) depends on temperature, because the solubility of O_2 in water changes with variations of temperature (Benson and Krause 1984; Melnichenko et al. 2008; Clever et al. 2014). Therefore, to take into account the influence of temperature on the outflow of electrons from PSI to O_2, we consider here the temperature dependence of O_2 solubility in water (Fig. 1d).

In this work, we do not consider the cyclic flow of electrons around PSI, in which electrons return from Fd^- via the water-soluble ferredoxin and ferredoxin-quinone reductase (FQR) to the ETC segment between PSII and PSI (at the PQ level). This is because Class B chloroplasts lose the

water-soluble ferredoxin, a mediator of the cyclic electron transport around PSI (Bendall and Manasse 1995; Strand et al. 2016).

Proton transport and ATP synthesis

We consider that protons accumulate inside the thylakoid lumen due to water oxidation by WOC and PQH_2 oxidation by the Cyt b_6f complex. The overall balance of the electron and proton transport in PSII is the following: two protons evolve in the lumen per one H_2O molecule decomposed in PSII; two electrons extracted from one H_2O molecule are used to reduce PQ to PQH_2. Oxidation of one PQH_2 molecule by the Cyt b_6f complex is accompanied by the release of two protons into the lumen. Note that the stoichiometric ratio $PQH_2/2H^+ = 1$ is true if the Q-cycle in the Cyt b_6f complex is neglected. We do not consider the operation of the Q-cycle, because of the absence of soluble ferredoxin in class B chloroplasts. Otherwise, two protons are released into the lumen per one electron transferred from PQH_2 to PSI (Mitchell 1976; Baniulis et al. 2008; Cramer and Hasan 2016; Tikhonov 2018). The overall electron and proton balance is the following: $H_2O + PQ + 2H^+_{out} \rightarrow 1/2O_2 + PQH_2 + 2H^+_{in}$. We also take into account that hydrogen ions translocated into the lumen can bind to the proton-accepting (buffer) groups, the concentrations of which significantly (by two orders of magnitude) exceed the concentration of electron carriers (for details, see Tikhonov and Blumenfeld 1985; Tikhonov and Vershubskii 2014, 2017).

The efflux of protons from the lumen is considered to occur through the ATP synthase (the proton flux J_{ATP}) and due to the passive leak of protons through the thylakoid membrane (the proton flux J_{pass}).

The proton flux coupled to ATP synthesis (J_{ATP})

The ATP synthase is a reversible molecular machine operating in both directions, either to form ATP from ADP and P_i (the endergonic process) or to hydrolyze ATP (the exergonic reaction). In Fig. 3, panel a schematically depicts the architecture of the ATP synthase ensemble: the membrane fragment of the ATP synthase complex (CF_0) is surrounded by the membrane lipids, the CF_1 fragment is exposed to stroma. Similarly to the model described earlier (Tikhonov and Vershubskii 2014; Vershubskii et al. 2017), we consider the proton flow as a two-step process: (1) the proton binding to the membrane-buried carboxy group ($–COO^- + H^+_{in} \rightarrow –COOH$) and (2) the proton dissociation from the protonated group –COOH ($–COOH \rightarrow –COO^- + H^+_{out}$) (Fig. 3b). The proton transfer through the ATP synthase proceeds via the carboxy groups located in the center moiety of the subunits *c*, which are assembled as the c_n-ring buried into the membrane (Fig. 3a). The transmembrane pH difference ($\Delta pH = pH_{out} - pH_{in}$) provides the protonation/deprotonation reactions shown in Fig. 3b, thereby supporting directed transfer of protons $\left(H^+_{in} \rightarrow H^+_{out}\right)$.

The ΔpH-driven proton transfer through the ATP synthase is coupled to directed rotation of the c_n-ring within the membrane (Junge et al. 1997; Fillingame et al. 2000; Diez et al. 2004; Ariga et al. 2007; Romanovsky and Tikhonov 2010; Junge and Nelson 2015). Rotating due to the energy of the *trans*-thylakoid pH difference, the c_n-ring actuates the operation of the coupling factor CF_1, catalyzing the ATP formation ($ADP + P_i \rightarrow ATP$). Figure 3c presents the typical pattern of the "flux–force" relationship (J_{ATP} *vs* ΔpH) related to the proton translocation through CF_0 at different values of the proton-motive force ΔpH. J_{ATP} is calculated for $pH_{out} = 8$ and $pK_a = 7.3$, where pK_a characterizes proton-accepting properties of Glu71 in subunits *c* of the c_n-ring (Vollmar et al. 2009). The equation for the flux J_{ATP} is presented in "Appendix 2" (Eq. A8). The sigmoid-type dependence of J_{ATP} *vs* ΔpH demonstrates that efficient flux J_{ATP} occurs after the generation of a sufficiently high ΔpH difference (> 1.5–2.0). We do not consider here the partitioning of *pmf* into ΔpH and $\Delta\psi$, because a steady-state difference in electric potentials $\Delta\psi = \psi_{in} - \psi_{out}$ in chloroplasts is negligible under the (quasi)steady-state conditions (Johnson and Ruban 2014; Davis et al. 2017).

One complete rotation of the c_n-ring results in the formation of three ATP molecules (Junge et al. 1997; Seelert et al. 2000; Junge and Nelson 2015). Bearing in mind that the rotation of the membrane-buried c_n-ring may depend on the fluidity of the membrane lipids surrounding c_n, we assume that the rate of ATP synthesis is controlled by the membrane fluidity. There are good reasons to believe that the acceleration of the c_n-ring rotation with temperature will stimulate the stoichiometric formation of ATP coupled to directed revolutions of the rotor. Therefore, we consider that the apparent rate constant $k_{ATP}(T)$, which stands in the equation describing ATP synthesis ("Appendix 1", Eq. A6), increases with temperature. We assume that the temperature dependence of $k_{ATP}(T) = \kappa_{ATP}(T) \cdot k^o_{ATP}$, where k^o_{ATP} is the model parameter related to $t_0 = 25$ °C, and $\kappa_{ATP}(T)$ is the temperature-dependent correction factor described by two exponents (Fig. 2c). The change-over of the apparent activation energy, corresponding to the inflexion in the Arrhenius plot of $k_{ATP}(T)$ at a characteristic temperature T_0, may be tentatively attributed to the structural changes in the membrane caused by the fluidization of the lipid domains surrounding the ATP synthase. Since the ATP synthase is the reversible enzyme capable of hydrolyzing ATP, we consider that the apparent rate constant of ATP hydrolysis is also the temperature-dependent process (see the temperature dependence of ATP hydrolysis in bean chloroplasts, "Appendix 3", Fig. 15). Within the framework of our model, we assume that the ratio of the rates of the forward (ATP synthesis)

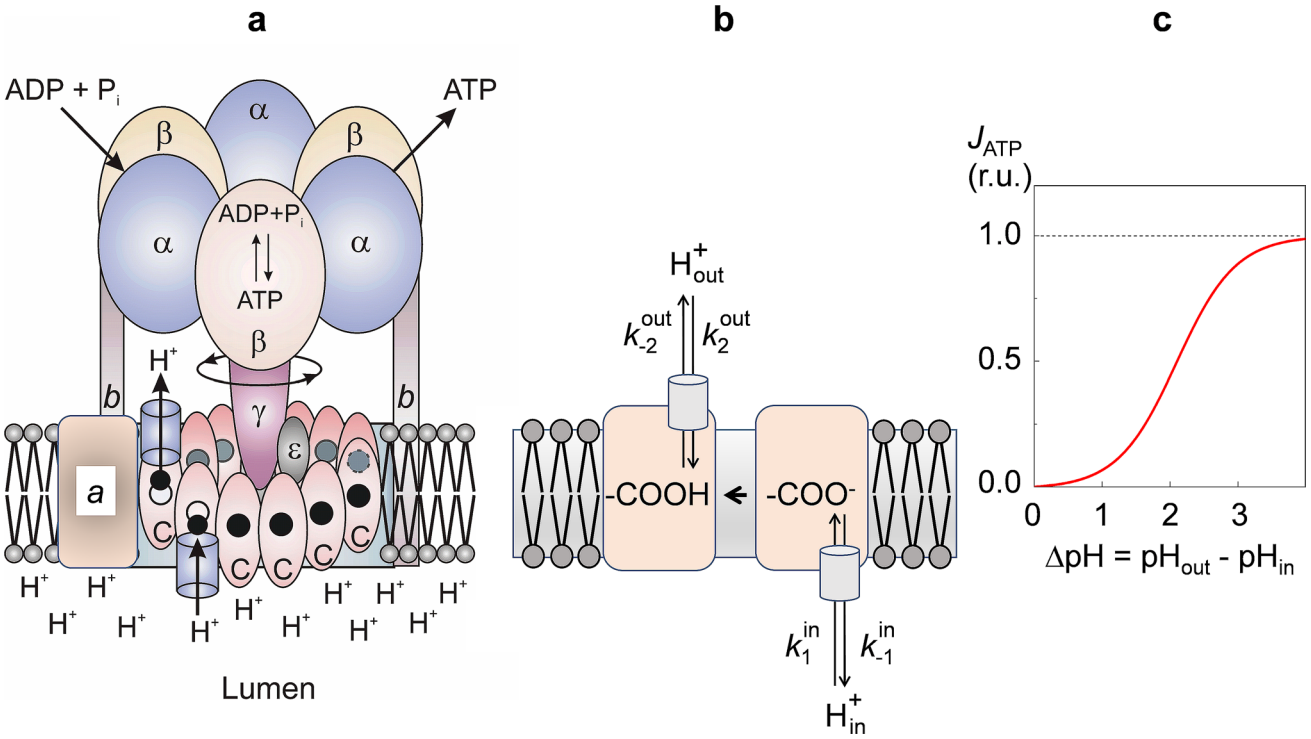

Fig. 3 Schemes illustrating the architecture of the ATP synthase ensemble (panel **a**) and the two-step mechanism modeling the transmembrane proton transfer (panel **b**). The transmembrane proton transfer, either through the ATP synthase (J_{ATP}) or passive flux (J_{pass}), occurs by means of the protonation/deprotonation exchange with the membrane-buried carboxy group. Panel **c** presents the force–flux relationship (J_{ATP} *vs.* ΔpH) calculated for the model parameter pK_c = 7.3 (see "Appendix 2" for details of J_{ATP} calculations)

and reverse (ATP hydrolysis) reactions may be taken as $k_{ATP}/k_{ADP} = 0.1$. This ratio was derived from the comparison of temperature dependences of the light-induced ATP synthesis and ATP hydrolysis in the dark in isolated bean chloroplasts (Timoshin et al. 1984; see also "Appendix 3" for the description of the measurements of ATP synthesis and ATP hydrolysis).

The passive flux of protons through the membrane (J_{pass})

Along with the active proton transport through the ATP synthase (J_{ATP}), the passive outflow of protons from the lumen (J_{pass}) will contribute to the establishment of ΔpH. For a proper choice of the function J_{pass}(ΔpH), we turned to experimental data on the H^+ ion uptake by thylakoids. Figure 4a shows the kinetics of light-induced acidification (pH$_{out}$ ↑) of weakly buffered suspension of chloroplasts in metabolic state 4 (Tikhonov et al. 1983). Figure 4b depicts the temperature dependence of the proton uptake (ΔH^+), demonstrating that ΔH^+ increases with the rise of temperature in the range 0–25 °C, but monotonously decreases at higher temperatures. The bell-like temperature dependence of ΔH^+ can be explained by the interplay of two effects: (i) the enhancement of proton pumping into the lumen due to the speeding-up of electron transport with temperature, and (ii) the acceleration of proton leak from the lumen caused by the membrane fluidization at sufficiently high temperatures.

The post-illumination decay of pH$_{out}$ reflects the proton leak from the lumen. In analogy to the model of the proton flow through the ATP synthase (Fig. 3b), we consider that the passive flux of protons through the membrane (J_{pass}) occurs by means of the proton exchange with the membrane-bound acidic groups (Vershubskii et al. 2011). For correct choice of the model parameters that determine J_{pass}, we compared the calculated values of J_{pass} with the appropriate experimental data obtained for isolated bean chloroplasts. As a touchstone for fitting the model parameters, we used the experimental curve measured in state 4 (without the addition of ADP). In this case, we could exclude the overestimation of J_{pass} that might occur due to the ATP synthase activity. Figure 4c shows the normalized semilogarithmic plots of the proton flux J_{pass} vs. temperature borrowed from experimental (stars) and calculated (circles) data. Experimental values were determined as $J_{pass} \sim 1/\tau_{1/2}$, where $\tau_{1/2}$ is the half-time of the post-illumination decay of pH$_{out}$ in state 4 (for definition, see Fig. 4a). Note that the experimental dependence demonstrates the characteristic inflexion of J_{pass} at $t_0 \approx 25$ °C. In accordance with experimental data, the calculated rate of the proton leakage (the passive flux J_{pass}) notably increased with the rise of temperature up to 25 °C.

At temperatures higher than t_0, the rate of the proton leakage also increased with temperature, but less significantly. Theoretical values of J_{pass} were determined as $J_{pass} = k_{H^+}(T) \cdot ([H^+_{in}] - [H^+_{out}])$, where the temperature-dependent coefficient $k_{H^+}(T)$ determines the *trans*membrane proton flux driven by the "proton force", $[H^+_{in}] - [H^+_{out}]$. The function $k_{H^+}(T)$ was parametrized by fitting calculated values of J_{pass} to experimentally measured proton fluxes determined for chloroplasts in the metabolic state 4 (compare experimental and theoretical data in Fig. 4c). In this work, we have considered three models of the temperature-dependent correction factor for the passive leak of protons, $k_{H^+}(T) = \kappa_{pass}(T) \cdot k^o_{pass}$, where k^o_{pass} is the normalizing coefficient related to temperature $t_0 = 25$ °C (Fig. 2d).

The calculated temperature dependence adequately reproduces the experimental data on the proton leak in the temperature range 10–35 °C, demonstrating the inflexion at 25 °C. Thus, following experimental data presented in Nolan (1981) and Tikhonov et al. (1983), we could suggest that the temperature dependence of the function J_{pass} has two branches described by different apparent activation energies.

Simulation of the membrane fluidity effects on structure–function relationships in thylakoids

In the context of the problem of structure–function relationships, observed upon the comparison of the functional (electron transport, proton translocation, and ATP synthesis) and structural characteristics of thylakoid membranes, it was interesting to consider the models, which differ with respect to the temperature-dependent patterns of partial photosynthetic reactions. We have considered the models characterized by different values of parameter t_0 related to the inflexion (break) points of temperature dependence of partial photosynthetic reactions, which are assumed to reflect the temperature of structural transitions in the lipid domains of thylakoid membranes. Figure 2 visualizes our choice of the temperature-dependence plots of four temperature-dependent correction functions related to the break points at $t_0 = 20$, 25, and 30 °C. As a touchstone for the choice of these dependences we use experimental data (Tikhonov et al. 1980, 1981, 1983, 1984; Timoshin et al. 1984) on the study of partial temperature dependences of photosynthetic processes in class B chloroplasts isolated from bean leaves.

Results

Redox transients of P_{700}

P_{700} redox transients are indicative of the intersystem ETC activity. Taking into account a rapid diffusion of PQH_2 in the membrane, and a high mobility of Pc within the lumen, one can conclude that it is the reaction of electron transfer from PQH_2 bound the quinone-binding portal of the Cyt b_6f complex that determines the overall rate of PQ turnover

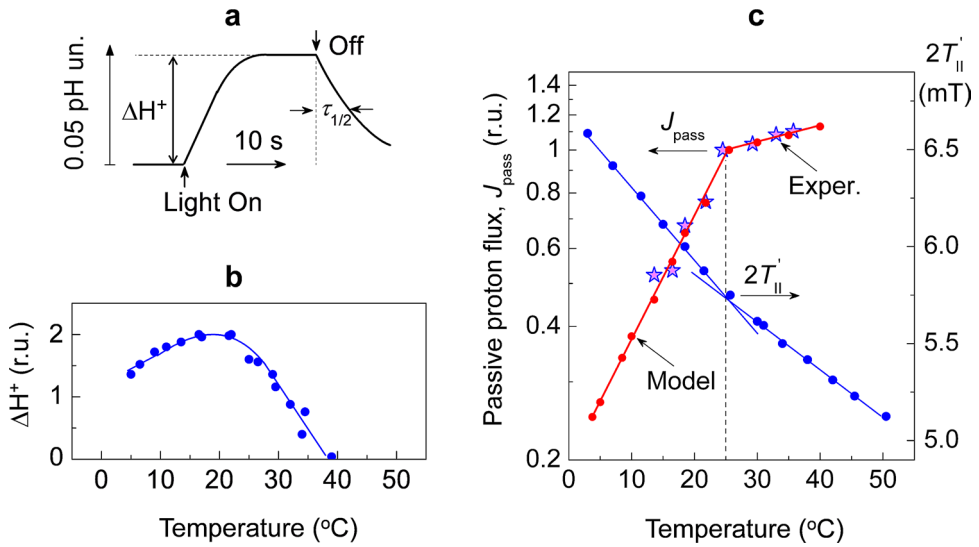

Fig. 4 Passive proton transfer through the thylakoid membrane. Panel **a** depicts the kinetics of light-induced pH changes in the weakly buffered suspension of chloroplasts in metabolic state 4. Panel **b** shows the temperature dependence of the light-induced uptake of proton (parameter ΔH^+). In panel **c**, we compare the normalized temperature dependences of semilogarithmic plots of the proton flux J_{pass} obtained in experiment (stars) and theory (circles), on the one hand, the structural parameter $2T'_{II}$ derived from the EPR spectrum of the lipid-soluble spin-probe 5-SASL (see text for more explanations). Experimental data are from Tikhonov et al. (1983)

between PSII and PSI (for references, see Tikhonov 2014, 2018). Indeed, over a wide range of experimental conditions (pH, ionic strength, and temperature), the processes of Q_B reduction to Q_BH_2 in PSII, PQH_2 dissociation from PSII and its diffusion across and along the thylakoid membrane towards the Cyt b_6f complex take less time than PQH_2 oxidation in the quinone-binding center Q_o (Tikhonov et al. 1984). Within the Cyt b_6f complex, electron transfer from the reduced iron–sulfur protein (ISP_{red}) to Cyt f proceeds more rapidly ($t_{1/2} \leq$ 2–4 ms, Gong et al. 2001; Yan and Cramer 2003) than PQH_2 oxidation ($PQH_2 \rightarrow$ ISP, $t_{1/2} \sim$ 10–20 ms, Stiehl and Witt 1969; Witt 1979). This suggests that namely the rate of PQH_2 oxidation after the formation of the substrate–enzyme complex (PQH_2-ISP_{ox}) determines the overall rate of electron transfer from PQH_2 to PSI.

As we noted above, the intersystem electron transport is governed by the light-induced changes in the lumen pH (pH_{in}). The light-induced acidification of the lumen causes the deceleration of PQH_2 oxidation by the Cyt b_6f complex, thereby reducing the rate of the intersystem electron transfer. The down-regulation of electron transport, caused by a decrease in pH_{in}, is associated with the back-pressure of the *intra*-thylakoid hydrogen ions on the proton-coupled oxidation of PQH_2 by the Cyt b_6f complex (for references, see Tikhonov 2014). Within the framework of our model, we take into account the influence of pH_{in} on the rate of PQH_2 oxidation ("Appendix 3", Fig. 13). pH-dependent regulation of the intersystem electron transport in chloroplasts manifests itself in the kinetics of the light-induced redox transients of P_{700} (Tikhonov et al. 1981; Vershubskii and Tikhonov 2020). Below we consider the results of modeling electron transport in class B chloroplasts in more details.

Kinetics of the light-induced redox transients of P_{700}

Figure 5 presents calculated time-courses of P_{700} redox transients induced by "Light 1" and "Light 2". In agreement with experimental data (Tikhonov et al. 1981), "Light 1" induces oxidation of P_{700}. Change-over from "Light 1" (exciting preferentially PSI) to "Light 2" (efficiently exciting both PSI and PSII) causes a decrease in $[P^+_{700}]$ due to electrons donated by PSII. The steady-state concentration of P^+_{700} and the rate of the post-illumination reduction of P^+_{700} depend on the metabolic state of chloroplasts. The kinetic curves presented in Fig. 5 are calculated for three metabolic states: state 3 (active functioning of the ATP synthase), state 4 (without ADP), and state 5 (uncoupled chloroplasts, $\Delta pH = 0$). The P^+_{700} level is maximal in state 4, when the oxidation of PQH_2 is retarded due to a sufficiently strong acidification of the lumen. In state 3, the P^+_{700} level is reduced. This is because the efflux of proton through the ATP synthase causes a certain decrease in ΔpH, thereby accelerating the intersystem electron flow. In uncoupled chloroplasts (state 5, $\Delta pH = 0$), rapid electron flow to P^+_{700} leads to more significant decrease in $[P^+_{700}]$. In states 3 and 5, the post-illumination reduction of P^+_{700} occurs much more rapidly than in state 4.

Effects of temperature on redox transients of P_{700}

The short-term mechanism of the temperature influence on the intersystem electron transport can be realized in several ways. One of the mechanisms represents a general influence of the temperature variations on the activity of partial chemical reactions that can be approximated by the Arrhenius law. Another mechanism may be related to temperature-dependent structural changes in the thylakoid membrane: variation of temperature may affect the membrane fluidity, for example, accelerating (or slowing down) diffusion of PQ and PQH_2 molecules in the lipid moiety of the membrane. The acceleration (or deceleration) of PQH_2 oxidation in the quinone-binding portal within the Cyt b_6f complex may be controlled by the physical state of the thylakoid membrane. PQH_2 oxidation is the proton-coupled electron transport process associated with the release of two protons into the lumen. The temperature-induced acceleration of proton dissociation from PQH_2 through the proton-conducting channels within the Cyt b_6f complex will promote the oxidation of PQH_2.

Figure 6 presents the temperature plots of the kinetic parameter $\tau_{1/2}$ (panel a) and the Arrhenius plots of its reciprocal value $\tau^{-1}_{1/2}$ (panel b), computed for the metabolic states 3, 4, and 5. Parameter $\tau_{1/2}$ is the half-time of the post-illumination reduction of P^+_{700}; its reciprocal value ($\tau^{-1}_{1/2}$) characterizes the overall rate of electron flow from PQH_2 to P^+_{700}. Temperature dependences of the kinetic parameters $\tau_{1/2}$ and $\tau^{-1}_{1/2}$ adequately describe the experimental plots (Tikhonov et al. 1980, 1984). At any given temperature, $\tau_{1/2}$ has the highest value in state 4 ("photosynthetic control", maximal ΔpH), and the lowest value in state 5 ($\Delta pH = 0$). This difference is explained by the retardation of PQH_2 oxidation caused by acidification of the lumen. The half-times of P^+_{700} reduction in the states 3 and 5 (at temperatures above 25 °C) are in the range $\tau_{1/2} \approx$ 15–20 ms (Fig. 6a). We note that similar values of $\tau_{1/2}$ were reported for isolated spinach chloroplasts (Stiehl and Witt 1969; Haehnel 1973, 1976, 1984), and bean chloroplasts (Tikhonov et al. 1981, 1984). In Fig. 6b we also present the kinetic data in the form of the Arrhenius plot, which is traditionally used to evaluate the activation energies of biochemical reactions. Figure 6b shows that in all metabolic states the temperature dependences of electron transfer to PSI reveal characteristic inflexions at $t_0 \approx$ 25 °C. The low-temperature and the high-temperature branches of the temperature dependence of parameter $\tau^{-1}_{1/2}$ are characterized by different activation ener-

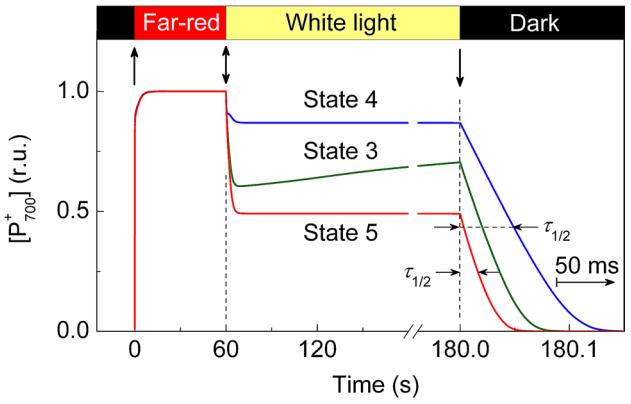

Fig. 5 Calculated time-courses of P_{700} redox transients (in metabolic states 3, 4, and 5) induced by the far-red light (FRL), exciting preferentially PSI, and white light (WL), efficiently exciting both PSI and PSII. Computer simulations refer to the standard model (parameter t_0 = 25 °C) and room temperature (25 °C)

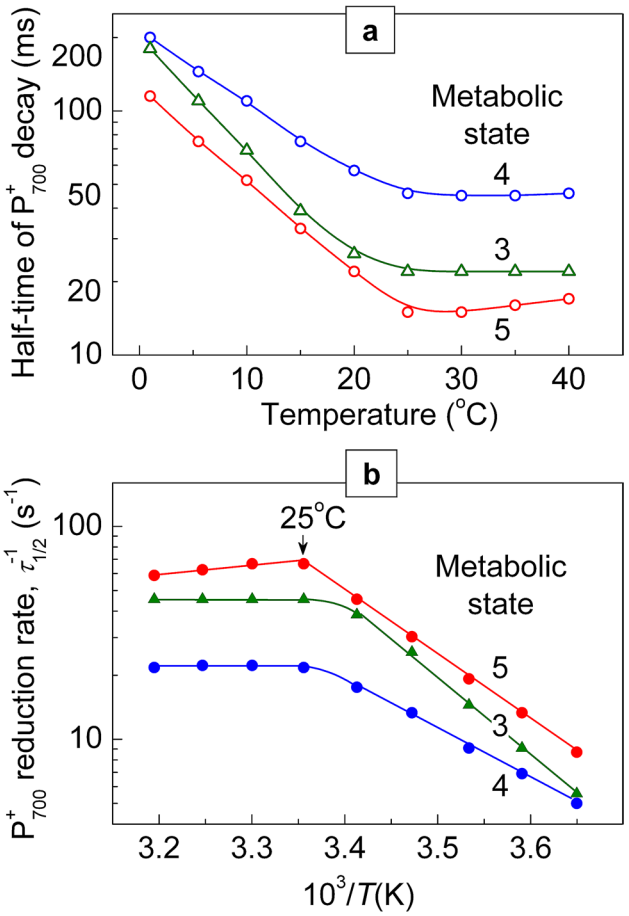

Fig. 6 Temperature dependences of the half-time $\tau_{1/2}$ of the post-illumination reduction of P^+_{700} (panel **a**) and the Arrhenius plot of its reciprocal value $\tau^{-1}_{1/2}$ (panel **b**) computed for metabolic states 3, 4, and 5, as indicated

gies, $E_a^{(1)}$and $E_a^{(2)}$, related to the temperature ranges below and above t_0, respectively. In the first case (below t_0), the exponential acceleration of electron transport with temperature is characterized by$E_a^{(1)}$ ~ 60 kJ mol^{-1}. At temperatures above t_0, the stimulating effect of temperature is insignificant or absent ($E_a^{(2)} \leq 3$ kJ mol^{-1}). This result may be accounted for by the interplay of different temperature-dependent factors that influence the electron flow from PQH_2 to PSI (via the Cyt b_6f complex and Pc).

The two branches of the Arrhenius plot of $\tau^{-1}_{1/2}$ can be explained by the balance of two effects: (i) a general activation of the apparent rate of PQH_2 oxidation by temperature, which dominates in the range of temperatures below t_0, and (ii) a decrease in $[PQH_2]$ and structural transitions in the lipid domains of the membrane (above t_0). Both factors are pre-determined by parametrization of the function $k_Q\left([PQ],[Pc],[H^+_{in}], T\right)$ and the model parameters $\xi(T)$ and $\kappa_{PSII}(T)$ (Section "Effects of temperature on the partial reactions of electron transport in thylakoids"). The rate of the oxidation of PQH_2, which donates electrons for the post-illumination reduction of P^+_{700} centers, will be proportional, at first approximation, to the product $\left[PQH_2\right] \cdot \left[b_6f\right]_{ox}$, where $[b_6f]_{ox}$ stands for oxidized Cyt b_6f complexes. This relationship suggests that the initial rate of the post-illumination reduction of P^+_{700} will depend on the plastoquinol concentration ($[PQH_2]$) at the moment of switching the light off.

Figure 7 shows the temperature influence on the steady-state concentrations of P^+_{700} (panel a) and PQH_2 (panel b). It is remarkable that, in the states 3 and 4, $[P^+_{700}]$ changes insignificantly with temperature, while the concentration of PQH_2 drops dramatically at temperatures above 30 °C. Thus, at high enough temperatures (> 30 °C) the electron flow from PQH_2 to PSI will not increase with temperature. This is the reason for relatively low $E_a^{(2)}$ values (< 3.5 kJ mol^{-1}). Note that in state 5, the Arrhenius plot of $\tau^{-1}_{1/2}$ at t > 30 °C formally shows negative $E_a^{(2)}$. It is highly likely that this is the manifestation of both factors: a decrease in the concentration of PQH_2, and an accelerated decay of $\left[P^+_{700}\right]$.

Acidification of the lumen ($pH_{in}\downarrow$) is an essential factor of the electron transport control in chloroplasts (for reviews, see Tikhonov et al. 1981; Kramer et al. 1999; Tikhonov 2012, 2013). Figure 7c displays the computed steady-state pH_{in} values in different metabolic states. In state 4 (when the overall proton flux through the CF_0 complex is virtually zero), pH_{in} decreases more significantly than in state 3 (when the protons located in the lumen can escape via the active CF_0–CF_1 complexes). In both states 3 and 4, the lumen becomes less acidic with increasing the temperature. This can be explained by the temperature-dependent acceleration of the proton outflow from the lumen through the ATP synthase and passive proton flux.

Summing up the above results, we conclude that the two branches of the temperature dependence of the rate of the post-illumination reduction of P^+_{700} may be explained by the interplay of two factors that influence the overall rate of the electron flow from PQH_2 to PSI. First, at sufficiently high temperatures (≥ 20–25 °C), occurs the depletion of the pool of reduced PQH_2 molecules (Fig. 7b), which serves as a source of electron donors transferred to P^+_{700} (via the Cyt b_6f complex and Pc). This causes the slowing down of the overall electron flux to PSI. Secondly, the inflexion in the plot of the temperature dependence may also reflect *thermo*-induced structural changes in the thylakoid membranes. The assumption about the temperature-dependent "structure–function" relationship was laid down upon the parametrization of the function $k_Q\left([PQ],[Pc],[H^+_{in}], T\right)$ according to (Eq. 2).

Electron transport coupled to ATP synthesis

Here we consider the relationship between the non-cyclic electron flow around PSI and ATP synthesis in thylakoids. Figure 8a presents the temperature dependences of steady-state electron fluxes from Fd^- to O_2 ($J_{Fd–O2}$) established in the metabolic states 3, 4, and 5, as calculated for our basic model (t_0 = 25 °C). These plots have bell-like shapes, with the maxima at 25 °C. The most intensive electron flow to O_2 ($J_{Fd–O2}$) occurs in uncoupled chloroplasts (state 5, ΔpH = 0), when the intersystem electron flow is not retarded by the lumen acidification. In states 3 and 4, the $J_{Fd–O2}$ fluxes are reduced due to the ΔpH-dependent retardation of the intersystem electron transport. In Fig. 8b we compare the temperature dependences of V_{ATP} (the rate of ATP formation) and $J_{Fd–O2}$ (the rate of electron transport). The ratio $V_{ATP}/J_{Fd–O2}$ corresponds to the experimentally measured P/2e ratio (also termed as the ATP/O ratio), which is conventionally used as a measure for the energy coupling efficiency in bioenergetic systems (Chance and Williams 1956; Mitchell 1976; Ivanov 1993; Rigoulet et al. 1998). Experimentally determined P/2e ratio also increases with temperature, reaching the value ≈ 0.8–1.2 at 22–25 °C (depending on experimental conditions), but remains constant at higher temperatures (Timoshin et al. 1984; see also Fig. 15 in "Appendix 3"). The rise of P/2e can be explained, at least partly, by temperature-induced activation of the ATP synthase. In our model, this factor is tacitly considered by the assumption that the model parameter $k_{ATP}(T)$ increases with temperature. The ratio P/2e depends on the conditions in which the chloroplasts are isolated and their properties are assayed (Reeves et al. 1972; Heise and Harnischfeger 1978; Ivanov 1993). It is also conceivable that the composition of the membrane lipids may affect ATP synthesis, due to their influence on the H^+ ion translocation from the proton pumps to the proton sinks (the CF_0 part of the ATP synthase).

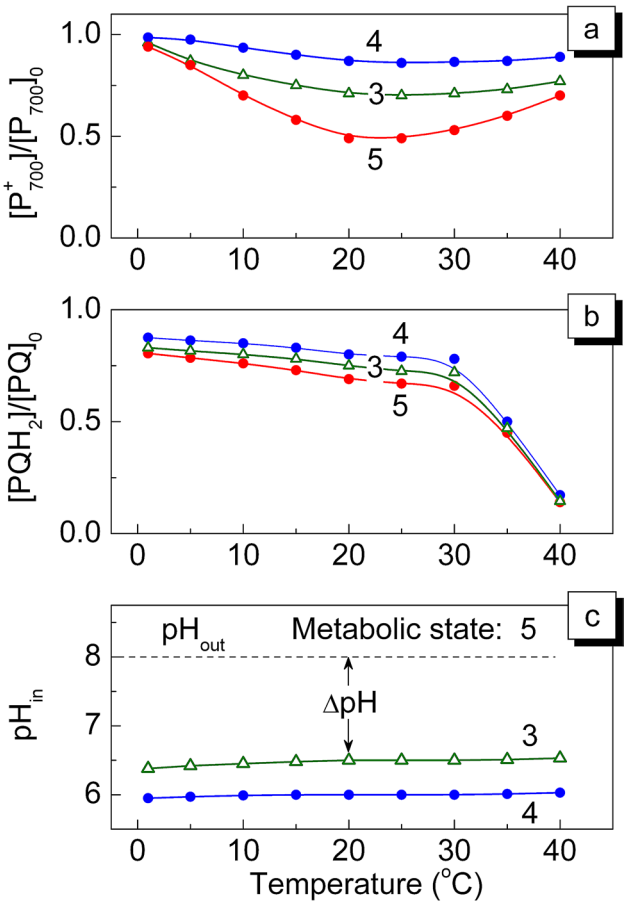

Fig. 7 Steady-state concentrations of P^+_{700} (panel **a**) and PQH_2 (panel **b**), and acidification of lumen pH_{in} (panel **c**), computed for metabolic states 3, 4 and 5, as indicated. Computer simulations refer to the standard model (t_0 = 25 °C)

Experimental studies show significant variability of photophosphorylation temperature dependences in chloroplasts isolated from the leaves grown under different experimental conditions (Yamori et al. 2014). Below we consider experimental data on bean chloroplasts, for which we observed the correlation between the temperature dependences of photophosphorylation and fluidity of membrane lipids (for references, see Kukushkin and Tikhonov 1988; Tikhonov and Subczynski 2005; Tikhonov 2020). In our earlier works (Tikhonov et al. 1980, 1983, 1984; Timoshin et al. 1984; Lutova and Tikhonov 1983, 1988), lipid-soluble derivatives of nitroxide radicals were used as the paramagnetic probes for *thermo*-induced structural changes in thylakoid membranes. Spin-labeled derivative of stearic acid, 5-SASL (Fig. 9a) is one of the most convenient probes for structural transients in the lipid domains of thylakoid membranes. Spin-probe molecules are intercalated in the membrane with the hydrophilic part in the polar headgroup region of the membrane. The radical mobility and ordering with respect to fatty acid chains of lipids depend on the position of the

nitroxide radical. Alkyl chains of the lipid bilayer portion of the thylakoid membrane are very well ordered in the near polar headgroup region and fairly fluid in the membrane center. The EPR spectra of 5-SASL reflect the mobility and ordering of its nitroxide fragment in the lipid domains of the membrane (Ligeza et al. 1998). When dissolved in the thylakoid membranes, 5-SASL gives the EPR spectrum (Fig. 9b) typical of nitroxide radicals located in a hydrophobic membrane environment. The rotational mobility of the nitroxide fragment influences the spectral parameters $2T'_{II}$ and $2T'_{\perp}$ of the EPR signal, which equal to the splitting of the "outer" and "inner" peaks (for definitions, see Fig. 9b). A degree of the nitroxide radical ordering in the lipid bilayer can be characterized by the so-called order parameter S, which can be calculated from the $2T'_{II}$ and $2T'_{\perp}$ parameters:

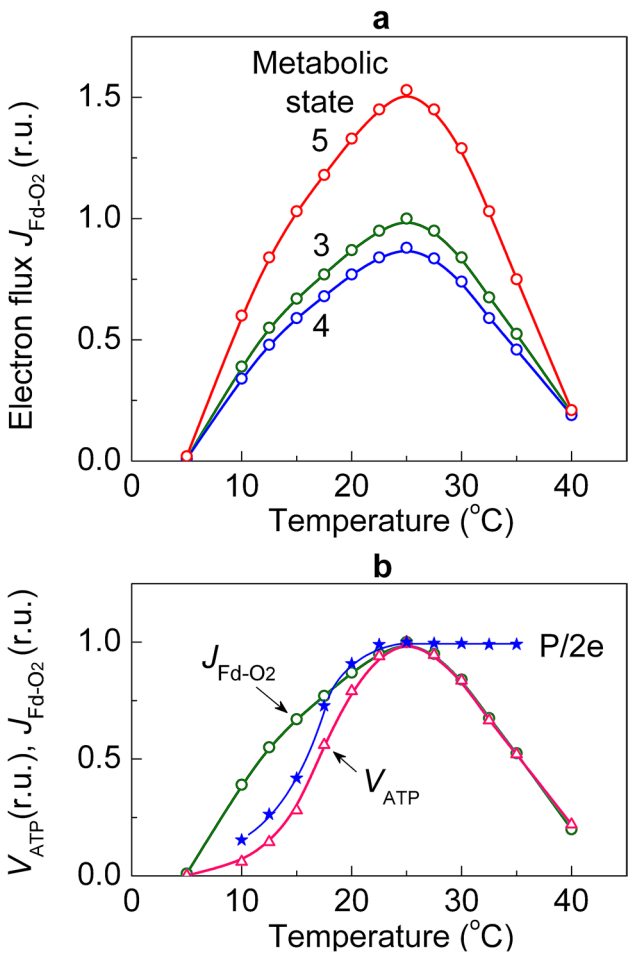

Fig. 8 Temperature dependences of steady-state electron fluxes from reduced ferredoxin (Fd^-) to O_2 (J_{Fd-O2}) established in metabolic states 3, 4, and 5 calculated for the basic model characterized by parameter t_0 = 25 °C (panel **a**). In panel **b** we compare the temperature dependence of V_{ATP} and J_{Fd-O2}; parameter P/2e = V_{ATP}/J_{Fd-O2} characterizes efficiency of coupling electron transport to ATP synthesis

$$S = h \cdot \left(T'_{II} - T'_{\perp}\right) / \left[T_{zz} - 0.5\left(T_{xx} + T_{yy}\right)\right],$$

where T_{xx}, T_{yy}, and T_{zz} are the main values of the hyperfine splitting tensor, and h is the correction factor for hydrophobicity of the local surrounding of the nitroxide radical (Berliner 1976; Griffith and Jost 1976; McConnell 1976). The order parameter S decreases with depth of the radical location in the thylakoid membrane (Ligeza et al. 1998). The S value is proportional to $2T'_{II}$, the value of which can be easily and reliably determined in a wide range of temperatures. Therefore, in most of our previous works, the spectral parameter $2T'_{II}$ was routinely used to assay temperature-induced changes in the membrane fluidity.

In Fig. 9 (panels c, d, and e) we compare the temperature dependences of the spectral parameter $2T'_{II}$ determined for spin-probe 5-SASL dissolved in thylakoid membranes of bean chloroplasts isolated from the leaves of different harvests (plants were grown under lower or higher temperatures; for more details, see Tikhonov et al. 1983; Kukushkin and Tikhonov 1988). All the plots of $2T'_{II}$ reveal characteristic inflexions ("breaks") of $2T'_{II}$ at different temperatures, at 25 °C (Fig. 9c), at 30 °C (Fig. 9d), and at 33 °C (Fig. 9e), suggesting that the *thermo*-induced "melting" of membrane lipids occurred at different temperatures. This may be caused, for example, due to different proportions of unsaturated and saturated fatty acids of the membrane lipids.

Experimental temperature dependences of ATP synthesis (V_{ATP}) show parabolic patterns: V_{ATP} increases with temperature, reaching the maximal value and then drops to zero. Note that the temperature corresponding to the inflexion in the plot of $2T'_{II}$ always coincides with the temperature at which the rate of ATP synthesis is maximal. A *thermo*-induced increase in V_{ATP} in the range of temperatures below t_0 is explained by the acceleration of electron transport and activation of the ATP synthase. At temperatures above t_0, V_{ATP} decreases with the rise of temperature. This may occur (i) due to a lessening of the electron flow from PSII to PSI, and (ii) due to an increase in the passive proton leak bypassing the ATP synthase. The temperature-induced increase in the membrane fluidity will accelerate electron transport and proton pumping into the lumen, on the one hand, while the acceleration of passive proton leakage (which bypass the ATP synthase) and the enhancement of ATP hydrolysis will suppress the ATP synthesis, on the other hand. As noted above, the maximal rates of the net ATP synthesis coincide with the temperatures of inflexion points in the plots of the "structural" parameter $2T'_{II}$. This observation can be considered as an evidence in favor of the regulatory role of the membrane fluidity in controlling the photosynthetic processes in thylakoids. It is highly likely that the proper balance between the gel (liquid-crystalline) and fluid phases in the thylakoid membrane, established at certain temperature, supports optimal conditions for efficient operation of

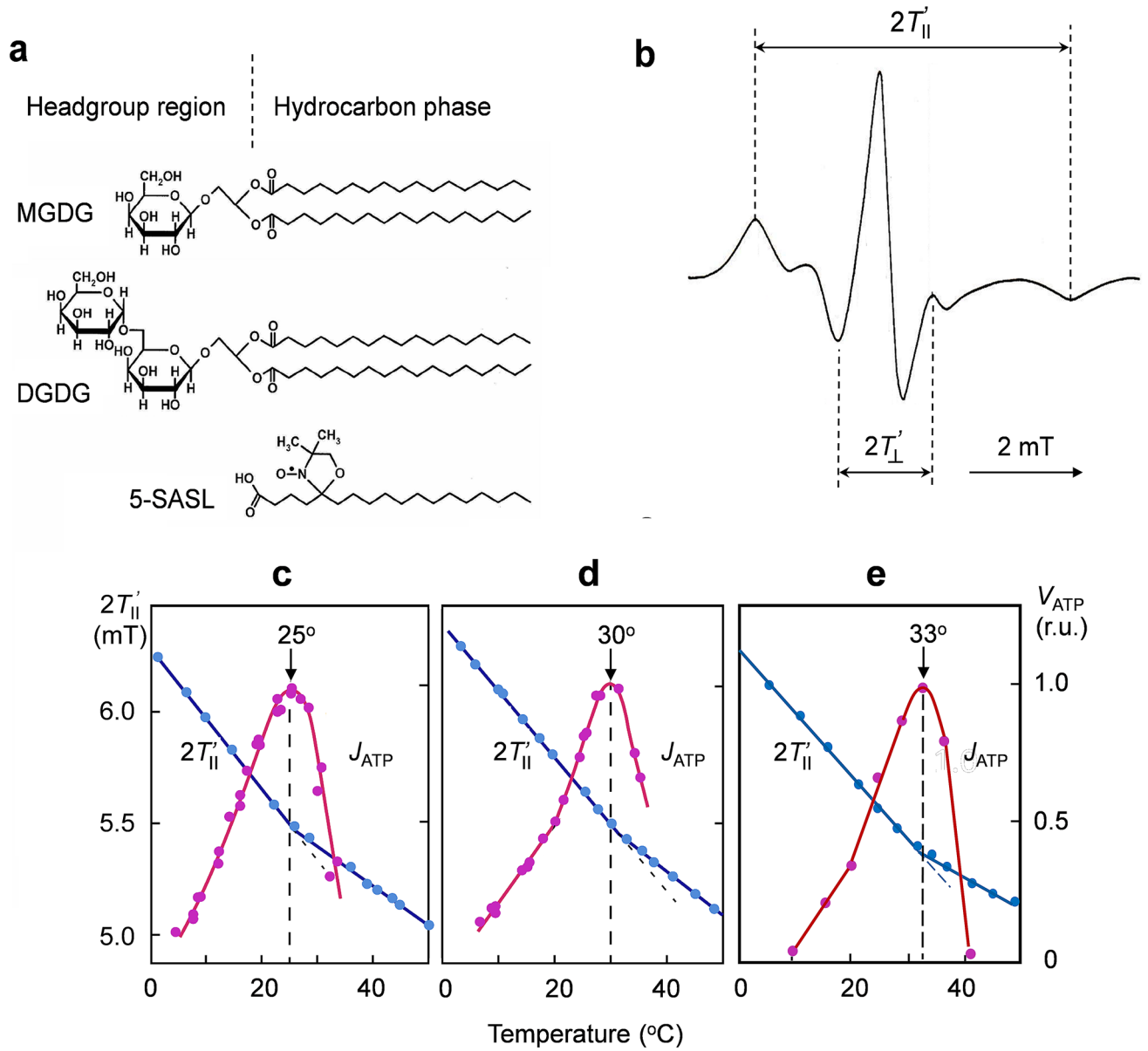

Fig. 9 Structure–function correlations in thylakoids. Panel **a** shows chemical structures of monogalactosyldiacylglycerol (MGDG), digalactosyldiacylglycerol (DGDG), and the stearic acid spin-probe 5 (5-SASL) used as an indicator of the membrane physical state (fluidity). Galactolipids (MGDG and DGDG) are major components of the lipid portion of thylakoid membranes. Spin label molecules are intercalated in the membrane with the hydrophilic part (left-hand side) in the polar headgroup region of the membrane. Panel **b** shows the EPR spectrum of 5-SASL dissolved in the thylakoid membrane at room temperature (modified from Ligeza et al. 1998; Tikhonov 2020). Panels **c**, **d**, and **e** show the correlations between the temperature dependences of the structural parameter $2T'_{II}$ and the normalized rate of ATP formation (V_{ATP}) in chloroplasts isolated from different batches of bean leaves (modified from Tikhonov et al. 1983; Kukushkin and Tikhonov 1988)

photosynthetic apparatus upon fluctuations of temperature (Tikhonov 2020).

The variability of temperature dependences of V_{ATP} observed in experiment can be modeled within the framework of our model. Figure 10 depicts calculated temperature dependences of V_{ATP} for the models, characterized by parameters t_0 = 20, 25, and 30 °C. Similar to experimental dependences, the calculated dependences $V_{ATP}(t)$ have the bell-like shapes. In accordance with experimental data, the model predicts that the temperature, at which calculated J_{ATP} values is maximal, coincides with the inflexion point at temperature t_0 characterizing the structural transition the thylakoid membrane (e.g., the so-called "melting" of the lipid bilayer). Thus, the model mimics the "structure–function"

mechanism of temperature-dependent regulation of photophosphorylation that could be realized by modulation of the membrane fluidity.

Discussion

In this work, we describe the results of the computer modeling of temperature-dependent regulation of photosynthetic processes in isolated thylakoids, and compare them to the relevant experimental data obtained earlier on isolated bean chloroplasts. Considering the sites of electron transport control, we have focused on the analysis of plastoquinone turnover between PSII and the Cyt b_6f complex, assuming that the reaction of PQH_2 oxidation is the rate-limiting step in the intersystem ETC. Rapid shuttling of PQ and PQH_2 between the PSII and Cyt b_6f complexes is determined by their relatively high mobility in the lipid domains of the membrane. The overall rate of the intersystem electron transfer is determined mainly by the rate of PQH_2 oxidation at the quinol-binding site (Q_o) localized in the interior of the Cyt b_6f complex, oriented towards the lumen. Close location of PSII and granal Cyt b_6f complexes, on the one hand, and sufficiently high fluidity of the membrane lipids, on the other hand, promote the formation of "substrate–enzyme" complex (PQH_2-b_6f), thereby accelerating the intersystem electron transport. The bifurcated reaction of PQH_2 oxidation starts with the transfer of one hydrogen atom from PQH_2 to the oxidized iron–sulfur protein (ISP_{ox}): PQH_2-ISP_{ox} → $PQH^{\bullet}$-$ISP_{red}H$. There are good reasons to believe that it is this step of PQH_2 oxidation that determines the overall rate of PQ turnover inside the Cyt b_6f complex (Crofts and Wang 1989; Hong et al. 1999; Crofts 2004; Crofts et al. 2000, 2013). Quantum chemical calculations (Ustynyuk and Tikhonov 2018) suggest that the activation energy of this reaction, $E_a \approx 60$ kJ/mol, is close to the apparent activation energy for electron transfer from PQH_2 to P^+_{700}. The effect of the membrane physical state (fluidity) on the rate of PQH_2 oxidation may be accounted for by the step of the proton dissociation from PQH_2 to the lumen (via the histidine residue of the ISP), which may have a restraining effect (Crofts et al. 2000).

The two branches of the temperature dependence of the post-illumination reduction P^+_{700} described by our model reflect the interplay of several processes. The inflexion in the temperature dependence of the rate of P^+_{700} reduction may have kinetic and structural reasons. Results of our calculations support this viewpoint. Considering the kinetic factor that determines the intersystem electron flow, we have to note that electron flow from PQH_2 to P^+_{700} (through the Cyt b_6f complex) will accelerate with the concentration of reduced PQH_2, i.e., $J_{QH_2 \rightarrow P^+_{700}} \sim [PQH_2]$ (Tikhonov and Vershubskii 2017; Suslichenko and Tikhonov 2019). The higher is the PQH_2 concentration, the faster electrons are delivered to P^+_{700}. A steady-state concentration of PQH_2 is determined by the balance between two processes: (1) the PQH_2 formation in PSII and (2) PQH_2 oxidation by the Cyt b_6f complex. The model predicts that $[PQH_2]$ gradually decreases at temperatures above 30 °C (Fig. 7b). Thus, a decrease in $[PQH_2]$ at sufficiently high temperatures, caused by the reduction of PSII activity, will hamper the intersystem electron flux through the Cyt b_6f complex, which will manifest itself as an apparent decrease in $E_a^{(2)}$.

Another reason for a decrease in $E_a^{(2)}$ at $t \geq 25$ °C may be associated with *thermo*-induced structural changes in thylakoids. Lipids provide the diffusion medium for PQH_2 molecules moving towards the PQH_2-binding portal located within the Cyt b_6f complex. The "solidification" of membrane lipids caused by a decrease in temperature (≤ 20–25 °C) should hamper the PQH_2 penetration into the quinone-binding portal in the Cyt b_6f complex, decelerating the PQH_2 oxidation. Otherwise, the membrane fluidization with the rise of temperature will accelerate the oxidation of PQH_2. An increase in the PQH_2 mobility in the membrane, caused by lipid fluidization at sufficiently high temperatures (≥ 25 °C), will promote the formation of the substrate–enzyme complex (PQH_2-b_6f) and accelerate the oxidation of PQH_2. However, after the transition of the most part of membrane lipids into the "fluid" state, the stimulating effect of temperature on electron transport will be masked by a decrease in $[PQH_2]$. Therefore, from the phenomenological viewpoint, a decrease in $[PQH_2]$ above sufficiently high temperatures ($> t_0$) will appear as a decrease in the apparent activation barrier $E_a^{(2)}$.

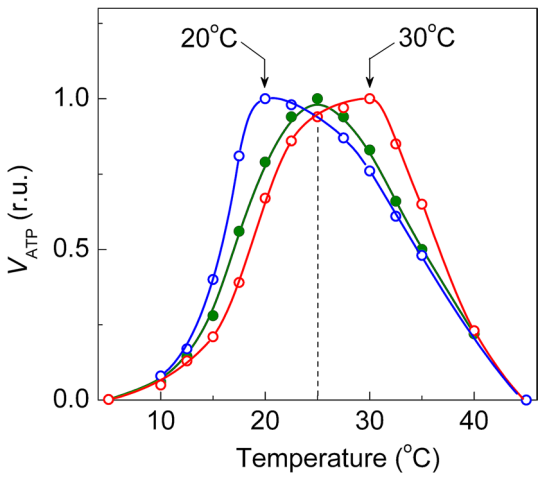

Fig. 10 Computed temperature dependences of the rate of ATP formation (V_{ATP}) for three models related to break points at $t_0 = 20$, 25, and 30 °C, respectively

Our line of arguments in favor of temperature-dependent modulation of the membrane fluidity as the regulatory factor in chloroplasts is based on experimental data on the structure-function relationships in thylakoids. The results of spin-probe studies of *thermo*-induced structural transitions in thylakoid membranes are in agreement with the notion that an adaptation of the photosynthetic apparatus of higher plants to changes in environmental temperature (Boardman 1977; Berry and Björkman 1980; Gounaris et al. 1984; Allen and Ort 2001) could be realized by fitting the fluidity of the lipid domains to an optimal level. Alterations in the membrane fluidity can be controlled by temperature-induced changes in the composition of unsaturated and saturated lipids in thylakoid membranes (Moon et al. 1995; Nie and Baker 1991). There is a rather strong evidence that the *thermo*-induced modulation of membrane fluidity markedly affects the rates of electron and proton transport processes in photosynthetic systems of oxygenic type (see Los et al. 2013; Yamori et al. 2014; Maksimov et al. 2017; Tikhonov 2020 and references therein). The coexistence of fluid and crystalline phases in photosynthetic membranes is believed to support physiologically relevant conditions (Moon et al. 1995; Schneider and Geissler 2013). The correspondence between the temperature dependences of kinetic and structural parameters in bean chloroplasts was demonstrated by the EPR method for chloroplasts isolated from the plants of various harvests (Tikhonov et al. 1983; Kukushkin and Tikhonov 1988). Changes in growth conditions (i.e., the cultivation temperature) caused similar changes in the inflexion point positions in the plots of $\tau_{1/2}^{-1}$ (the rate of P_{700}^{+} reduction) and spectral parameters of lipid-soluble spin probes. When plants were grown at reduced temperatures, the inflexion points drifted towards lower temperatures; at elevated growth temperatures, the inflexion points shifted towards higher temperatures. Taking into account the reproducible correlations between "kinetic" and "structural" parameters (Fig. 9, panels c, d, and e), one can conclude that the rate of the intersystem electron transfer is affected by the membrane fluidity. It is conceivable that "melting" of the membrane lipids, when the vast majority of lipid molecules are in the "fluid" state, would accelerate the substrate–enzyme complex (PQH_2-b_6f) formation. The light-induced pumping of proton into the lumen supports the ATP synthesis, while the *thermo*-induced disordering of the membrane lipids stimulates the passive proton leakage, which bypasses the ATP synthase (for illustration, see sketch in Fig. 11). The latter factor will reduce the net rate of ATP formation at high temperatures.

Below we consider two questions: (1) how the membrane fluidity could influence the rate of PQH_2 oxidation reaction, and (2) why the "fluidization" of the membrane causes an apparent decrease in the activation energy of electron transport processes ($E_a^{(1)} > E_a^{(2)}$)? As noted above, the rate of PQ turnover is determined predominantly by the intrinsic events within the Cyt b_6f complex: the penetration of PQH_2 into the quinone-binding site Q_o, and the subsequent oxidation of PQH_2, which is accompanied by the release of protons into the bulk of the lumen. In the catalytic site Q_o of the Cyt b_6f complex, PQH_2 is oxidized by the iron–sulfur protein (ISP), which accepts the H atom (electron + proton) from PQH_2. According to the "proton-gated" model of quinol oxidation (Brandt 1996; Link 1997), in order to create a sufficiently high reducing potential, the PQH_2 molecule must be deprotonated ($PQH_2 \rightarrow PQH^- + H^+$) before the first electron can be transferred to the oxidized iron–sulfur protein (ISP_{ox}). Both the electron and proton are transferred in concert to the Fe_2S_2 cluster of the ISP_{ox} and to the His residue of the ISP_{ox} (for references, see Crofts and Wang 1989; Crofts 2004; Osyczka et al. 2005; Cramer et al. 2006, 2011). Then the proton dissociates from the ISP_{ox} to the bulk of the lumen through a specific proton-conducting channel (Hasan et al. 2013a; Tikhonov 2014, 2018). Thus, taking into account that PQH_2 oxidation is the proton-coupled electron transport process associated with dissociation of H^+ ions into the lumen, we can suggest that the proton transfer through the membrane may serve as a factor controlling the rate of PQ turnover.

The operation of the ISP is associated with its conformational changes that might be another possible factor controlling the rate of PQH_2 oxidation. Extensive crystallographic disorder of the ISP extrinsic domain indicates its conformational mobility and flexibility (Hasan and Cramer 2012; Hasan et al. 2013b). The Fe_2S_2 cluster serves as the recipient of an electron donated by PQH_2 and then it donates the electron to Cyt *f*. After the reduction of the ISP, the mobile domain of the ISP_{red}, which contains the redox center (the Fe_2S_2 cluster), moves from the Q_o site towards the heme *f*. After the reduction of Cyt *f*, the oxidized Fe_2S_2 cluster returns the Q_o site. The roundtrip of the mobile domain of the ISP to heme *f* and back to the Q_o site can partly contribute to the turnover time of the Cyt b_6f complex. However, the structural and kinetic data suggest that the "tethered" movement of the mobile domain of the ISP is not a rate-limiting step for electron transfer inside the Cyt b_6f complex. The restricted diffusion of the ISP redox center occurs rapidly compared to the overall rate of PQH_2 oxidation. Electron transfer from the reduced ISP to Cyt *f* proceeds more rapidly ($t_{1/2} \leq$ 2–4 ms, Gong et al. 2001; Yan and Cramer 2003) than PQH_2 oxidation ($t_{1/2} \sim$ 10–20 ms; Stiehl and Witt 1969; Witt 1979). This means that the rate of PQH_2 oxidation is determined predominantly by the proton-coupled electron transfer after the formation of the substrate–enzyme complex (PQH_2-ISP_{ox}).

Lipids may play important role in operation of the Cyt b_6f complex. This complex encloses a cavity

(30 Å × 15 Å × 25 Å), which serves as the portal for PQH_2 binding to the catalytic center (Cramer et al. 2006). Inside the cavity, there were identified 23 lipid-binding sites per monomer of the dimeric b_6f complex from *Noctos* PCC 7120 (Hasan and Cramer 2014). It is conceivable that the neutral lipids localized inside the quinone-binding cavity may determine enhanced conformational flexibility of the ISP mobile domain. It is essentially in this context that lipids may play important role in regulation of electron transfer through the Cyt b_6f complex. In thylakoid membranes, most of the lipids are presented by galactolipids, which contain polyunsaturated fatty acids (Wada and Murata 2009; Zhou et al. 2016). Variations in the relative content of unsaturated fatty acids in thylakoid membranes were found to be one of the factors that control the photosynthetic activity of chloroplasts (Los and Murata 2004; Los et al. 2013; Maksimov et al. 2017). We may speculate that the "fluidization" of the thylakoid membrane will facilitate the proton transfer from PQH_2 to the bulk of the lumen, thereby stimulating the deprotonation of reduced $ISP_{red}H^+$ ($ISP_{red}H^+ \rightarrow ISP_{red} + H^+_{in}$) and further electron transfer from ISP_{red} to Cyt *f*. A rapid proton transfer into the lumen through the proton channels of the Cyt b_6f complex would accelerate the Cyt b_6f turnover. *Thermo*-induced conformational changes in the Cyt b_6f complex might also stimulate PQH_2 oxidation. Thus, the temperature-dependent release of diffusion barrier for protons and concomitant acceleration of PQH_2 oxidation should promote electron transfer between PSII and PSI. It is conceivable that after the temperature-dependent "melting" of the vast majority of thylakoid lipids (the "fluidization" of the membrane), the rate of the substrate–enzyme complex (PQH_2-b_6f) formation will depend on temperature, but not significantly.

Concluding remarks

1. For modeling of the photosynthetic electron transport processes in thylakoids, we consider that the processes of PQ turnover (reduction of PQ in PSII, diffusion of PQH_2 and its oxidation by the Cyt b_6f complex) determine the overall rate of electron transport between PSII and PSI. The rate-limiting step of the intersystem electron transport is associated with PQH_2 oxidation at the quinone-binding site of the Cyt b_6f complex. The overall rate of the intersystem electron transfer is determined mainly by the rate of PQH_2 oxidation at the quinol-binding site localized in the interior of the Cyt b_6f complex. The feedback control of PQH_2 oxidation is governed by the *intra*-thylakoid pH. Rapid shuttling of electrons between PSII and Cyt b_6f complexes by PQH_2 is determined by a high mobility of PQH_2 and PQ molecules within the lipid domains of the thylakoid membrane.

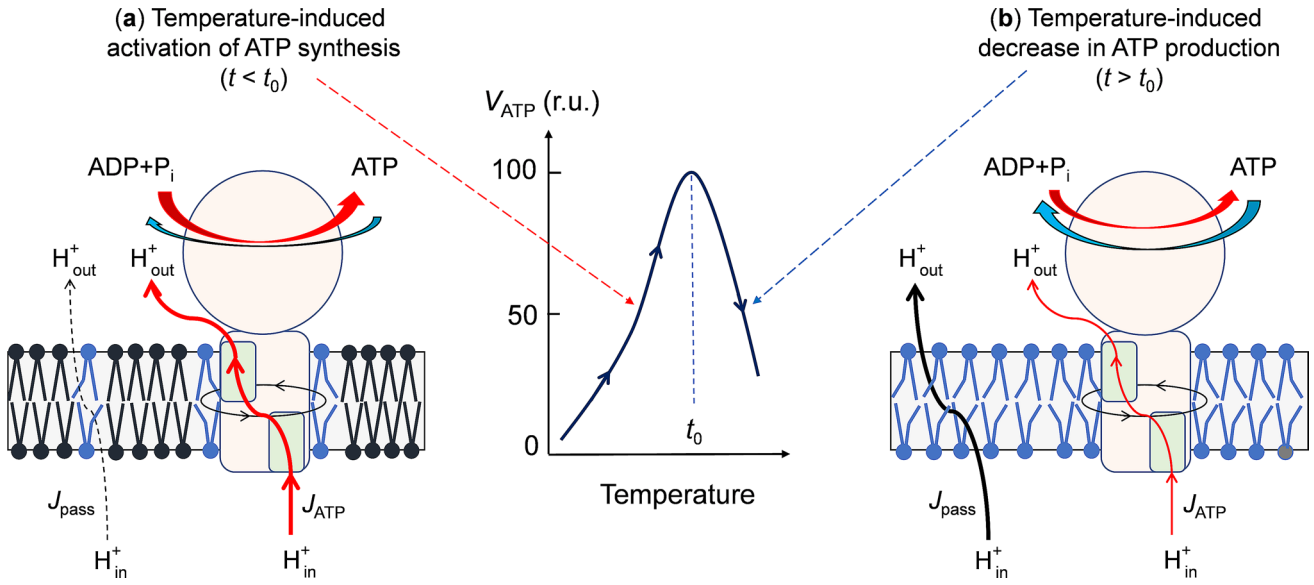

Fig. 11 A symbolic sketch qualitatively illustrating the effect of the redistribution of proton fluxes J_{ATP} and J_{pass} caused by temperature-induced structural changes in the physical state of the thylakoid membrane. Panel **a** reflects the up-regulation of the temperature dependence of ATP synthesis, $V_{ATP}(T)$. Stimulation of ATP synthesis occurs due to a general temperature-dependent activation of the ATP synthase, including the acceleration of the c_n-ring rotation in the lipid moiety with the temperature-induced fluidization of the thylakoid membrane. In this case, stimulation of ATP synthesis with temperature prevails over the loss of protons caused by their bypassing through the membrane. Panel **b** illustrates the down-regulation of ATP formation at sufficiently high temperatures, when temperature induces more significant leak of protons (J_{pass}) due to increasing the room of fluid domains in thylakoid membranes, thereby decreasing $V_{ATP}(T)$

2. Both the PQ/PQH_2 movement within the thylakoid membrane and PQH_2 oxidation within the Cyt b_6f complex are the temperature-dependent processes. Structural changes in the membrane are the clue factors of temperature-dependent regulation of photosynthesis. The intersystem electron transfer and related processes (e.g., proton pumping, ATP synthesis, and *trans*-thylakoid proton transfer) are controlled by the degree of membrane fluidity. The mechanism of fluidity-dependent regulation of photosynthetic processes is supported by correlations between the functional characteristics (electron and proton transport, ATP formation) and "structural" properties of the thylakoid membrane (i.e., membrane fluidity).
3. Computer modeling of electron and proton transport processes supports the notion that PQH_2 oxidation by the Cyt b_6f complex and the processes of *trans*membrane H^+ ion transfer are the basic temperature-dependent steps that determine the overall flux of electrons from PSII to molecular oxygen and the net ATP synthesis upon variations of temperature. Numerical experiments have demonstrated that the temperature dependences of these processes, which are sensitive to the physical state of the membrane, will determine the temperature-dependent pattern of PQH_2 oxidation.
4. The two branches of the temperature effect on the intersystem electron transport can be explained by (1) a general temperature effect on the activity of PSII, and the rate of PQH_2 oxidation by the Cyt b_6f complex, and by (2) *thermo*-induced structural changes in the thylakoid membranes, which can influence the proton transfer through the membrane, accelerating the proton leak with temperature. The low-temperature branch of activation of the intersystem electron transport ($E_a \sim 60$ kJ mol^{-1}) is explained by the temperature-dependent acceleration of PQH_2 oxidation. The attenuation of the activation effect at temperatures ≥ 25 °C can be explained by a gradual decrease in the concentration of PQH_2 and *thermo*-induced structural changes in thylakoid membranes.
5. The model describes the bell-like temperature dependence of ATP synthesis as resulting from the interplay of several factors: (1) the *thermo*-induced acceleration of electron transport through the Cyt b_6f complex, (2) a deactivation of PSII photochemistry at temperatures above the structural transient, and (3) an acceleration of the passive proton outflow from the thylakoid lumen, bypassing the ATP synthase complex, which is caused by an increase in the permeability of thylakoid membranes at temperatures above the structural transient. The model also describes the temperature dependence of experimentally measured parameter P/2e, which is determined as the ratio between the rates of ATP synthesis and pseudocyclic electron transport.

Summing up the results of our study, we can state that, though the model described above is simplified, it recapitulates many of the temperature-dependent responses observed in the thylakoids in vitro (isolated class B chloroplasts). In particular, the model describes two branches of the temperature dependences of pseudocyclic electron transport and the bell-like plot of the ATP formation versus temperature. The future work on the theoretical study of temperature dependences of photosynthetic reactions in chloroplasts will need the expansion of the model presented here, including the consideration of (1) the Mitchell's Q-cycle; (2) alternative electron transport pathways (non-cyclic/cyclic), (3) the light-induced redox regulation of the ATP synthase, and (4) the metabolism-related processes like the CBC reactions.

Acknowledgements We thank Dr. V.I. Priklonskii for the adjustment of the computer program in order to parameterize the constants of temperature dependences of the partial reactions of electron transport. Experimental studies on bean chloroplasts, used in this work for parametrization of the model parameters, were performed earlier by one of the authors in collaboration with Professor E.K. Ruuge, Professor G.B. Khomutov, and Dr. A.A. Timoshin. We are greatly thankful to all our colleagues and collaborators.

Author contributions ANT: design and supervision of the work, data processing, writing of the manuscript. AVV: computer calculations, data processing, discussion of results, preparation of the manuscript.

Funding This work was partly supported by the Russian Foundation for Basic Research (Grant 18-04-00214).

Compliance with ethical standards

Conflict of interest The authors declare no conflict of interest.

Appendix 1: equations and rate constants of the model

Equations (A1–A7) represent the system of ordinary differential equations (ODE), which describe the redox transitions of electron carriers (variables [Fd], $[P^+_{700}]$, $[P^+_{680}]$, [Pc], [PQ]), the acidification of the thylakoid lumen ($[H^+_{in}]$), and the yield of ATP (variable [ATP]).

$$\frac{d[\mathrm{Fd}]}{d\tau} = \left\{k_{\mathrm{Meh}}[O_2(T)]\right\} \cdot \left([\mathrm{Fd}]_0 - [\mathrm{Fd}]\right) - L_1 \cdot k_{P_{700}} \cdot [\mathrm{Fd}] \cdot \left([P_{700}]_0 - [P^+_{700}]\right) \quad (A1)$$

$$\frac{d[P^+_{700}]}{d\tau} = L_1 \cdot k_{P_{700}} \cdot [\mathrm{Fd}] \cdot \left([P_{700}]_0 - [P^+_{700}]\right) - k_{\mathrm{Pc}} \cdot [P^+_{700}] \cdot \left([\mathrm{Pc}]_0 - [\mathrm{Pc}]\right) \quad (A2)$$

$$\frac{d[\mathrm{Pc}]}{d\tau} = k_{\mathrm{Pc}} \cdot [P^+_{700}] \cdot \left([\mathrm{Pc}]_0 - [\mathrm{Pc}]\right) - k_{\mathrm{Q}}([\mathrm{PQ}],[\mathrm{Pc}],[H^+_{in}], T) \quad (A3)$$

Table 1 Characteristic times of partial reactions of electron transfer considered within the framework of the model and their comparison with experimental data

Electron transport processes described by the ODE A1–A7	Apparent rate constant ($k = 1/\tau$)	Characteristic time, τ (s) (room temperature)		References
		Model	Experimental data	
$H_2O \rightarrow P_{680}$	k_{H_2O}	10^{-4}	τ_{H_2O}~$2 \times 10^{-5} - 1.6 \times 10^{-3}$ (depending on the S_n-state of WOC)	Witt (1979), Meyer et al. (1989), Razeghifard et al. (1997), Dau and Haumann (2008) and Lubitz et al. (2019)
P680 → PQ	$k_{P_{680}}$	7×10^{-4}	$6 \times 10^{-4} - 10^{-3}$ (depending on the redox states of Q_A and Q_B in PSII)	Witt (1979), Haehnel (1984), de Wijn and van Gorkom (2001), Cardona et al. (2012)
$P_{700} \rightarrow Fd(F_A/F_B)$ (via A_1 and F_X)	$k^*_{P_{700}}$	7×10^{-4}	$\leq 5 \times 10^{-7}$ ($P^*_{700} \rightarrow F_A/F_B$) (laser pulse experiments)	Setif and Bottin (1994), Díaz-Quintana et al. (1998), Brettel and Leibl (2001) and Agalarov and Brettel (2003)
$Pc \rightarrow P_{700}$	k_{Pc}	2×10^{-4}	$(2–20) \times 10^{-5}$	Haehnel (1984), Sigfridsson (1998)
$Fd(F_A/F_B) \rightarrow MV \rightarrow O_2$	k_{Meh}**	$10^{-3} - 10^{-2}$***	~$10^{-3} - 10^{-2}$	Asada (1999), Kuvykin et al. (2008) and Milanovsky et al. (2017)

*Our choice of the $k_{P_{700}}$ value was determined by the following reasons. Within the framework of the model, the apparent rate constant $k_{P_{700}} = \tau^{-1}_{P_{700}}$, where $\tau_{P_{700}}$ is the characteristic time determined by the overall time of electron transfer from P_{700} to the terminal acceptors of PSI (F_A and F_B). According to the literature data obtained on the basis of laser pulse experiments (for references, see Díaz-Quintana et al. 1998; Brettel and Leibl 2001), the overall time of electron transfer from the excited center P^*_{700} to F_A and F_B takes ≤ 500 ns. However, during the action of the prolonged continuous light of saturating intensity exciting PSI, the maximal frequency of PSI turnover, determined by the average time between the successive acts of the light-induced electron donation from P_{700} to Fd, will be limited by the recovery of P^+_{700} to P_{700} due to the electron influx to P^+_{700} from Pc^- (τ_{Pc} ~ 20–200 μs; Haehnel 1984; Sigfridsson 1998). Bearing in mind that electron flow from PSII to PSI will also depend on the presence of the surplus amounts of PQ, we have taken the model parameter $\tau_{P_{700}}$ as 7×10^{-4} s. This value matches the value of the model parameter $\tau_{P_{680}}$, providing balanced (stoichiometric) electron flow from PSII to PSI under the steady-state conditions

**Parameter k_{Meh} is a variable model parameter, the value of which was adjusted semi-empirically, in order to provide the best fitting of the calculation results to experimental data on non-cyclic electron flow

***Note that this time is related to the reduction of the overall pool of O_2 molecules, the number of which is much higher than the number of PSI complexes, $[O_2]/[PSI]$ ~ 100–1000. Since the light-induced uptake of O_2 due to the Mehler reaction will be determined as $d[O_2]/d\tau = -k_{Meh} \cdot [O_2] \cdot [Fd^-]$, we find that the overall rates of electron transfer from PSI to O_2 (via MV) and the rate of O_2 consumption measured experimentally to be comparable by an order of magnitude

$$\frac{d[P^+_{680}]}{d\tau} = L_2 \cdot \xi(T) \cdot k_{P_{680}}(T) \cdot [PQ] \cdot \left([P_{680}]_0 - [P^+_{680}]\right) - k_{H_2O} \cdot [P^+_{680}] \tag{A4}$$

$$\frac{d[PQ]}{d\tau} = 0.5 \cdot k_Q([PQ],[Pc],[H^+_{in}], T) - 0.5 \cdot L_2 \cdot \xi(T) \cdot k_{P_{680}}(T) \cdot [PQ] \cdot [H^+_{out}] \cdot \left([P_{680}]_0 - [P^+_{680}]\right) \tag{A5}$$

$$\frac{d[ATP]}{d\tau} = \frac{k_{ATP}(T)}{m} \cdot \left([ADN]_0 - [ATP]\right) \cdot \frac{[H^+_{out}] \cdot [10^{\Delta pH} - 1]}{\alpha + [H^+_{out}] \cdot [10^{\Delta pH} + \beta]} - k_{ADP}(T) \cdot [ATP] \tag{A6}$$

$$\left[1 + \frac{K_M \cdot B_{in}}{(K_M + [H^+_{in}])^2}\right] \frac{d[H^+_{in}]}{d\tau} = k_{H_2O} \cdot [P^+_{680}] + 2 \cdot k_Q([PQ],[Pc],[H^+_{in}], T) - k_{H^+}(T) \cdot ([H^+_{in}] - [H^+_{out}]) - k_{ATP}(T) \cdot \left([ADN]_0 - [ATP]\right) \cdot \frac{[H^+_{out}] \cdot [10^{\Delta pH} - 1]}{\alpha + [H^+_{out}] \cdot [10^{\Delta pH} + \beta]} \tag{A7}$$

Here, the function $k_Q([PQ],[Pc],[H^+_{in}], T)$ describes the electron transfer from PQH_2 to Pc via the Cyt b_6f complex [see above Eqs. (1) and (2)]. ΔpH is the *trans*-thylakoid pH difference, $\Delta pH = pH_{out} - pH_{in}$. We assume that pH_{out} to be constant, $pH_{out} = 8$, due to sufficiently high buffer capacity of the outer medium. $[ADN]_0$ is the total concentration of ADP and ATP. The model parameters α and β in Eqs. (A6) and (A7) are determined by the rate constants of the proton exchange with the proton-accepting groups of the ATP synthase (see Fig. 3 and the explanations below). Formulating Eqs. (A1–A7), we assume the following stoichiometry between the electron transport and ATP synthase complexes: $[PSI]/[PSII]/[b_6f]/[CF_0\text{-}CF_1] = 1/1/1/1$. The relative capacity of the photo-reducible PQ pool, Fd, and Pc was taken as $[PQ]_0/[PSI] = 10$, $[Fd]_0/[PSI] = 3$, and $[Pc]_0/[PSI] = 1.5$, respectively.

The model parameters L_1 and L_2 describe the numbers of light quanta per unit time exciting P_{700} and P_{680}, respectively. Parameter m expresses the stoichiometry of proton transfer through the ATP synthase, H^+/ATP; $m = n/3 = 14/3$ is the stoichiometry ratio, the ratio between a number $n = 14$ of subunits c in the c_n-ring to three ATP molecules formed per one turn (360°) of the membrane rotor c_n (Seelert et al. 2000; Vollmar et al. 2009). Constants marked with a subscript "0" are the maximal concentrations of the relevant variables. Constants $k_{P_{680}}$, $k_{P_{700}}$, k_Q, k_{Pc}, and k_{Meh} are the effective rate constants of the reactions shown in Fig. 1. Constant k_{ADP} governs the effective rate of ATP hydrolysis. The function k_Q, which characterizes the oxidation of PQH_2, depends on pH_{in} (for details see Eqs. 1 and 2; Dubinskii and Tikhonov 1997; Vershubskii et al. 2011). The model parameters K_M and B_{in}, characterize the buffer properties of the system. Here, K_M is the equilibrium constant for the reaction of proton binding by buffer groups inside of thylakoids; the model parameter B_{in} is the concentration of these buffer groups. In this work, we assume the stoichiometric ratio $B_{in}/PSI = 100$ (for details, see Vershubskii et al. 2011). Note that parameters K_M and B_{in} (the left side of Eq. A7) can influence the time-course of the system response to switching the actinic light on. The steady-state levels of all the variables of the model, however, are independent on the K_M and B_{in} values (Dubinskii and Tikhonov 1997).

The formulation of the system of differential equations and the choice of the apparent rate constants have been considered in details in our previous works (Vershubskii et al. 2011, 2018). The rate constants for key stages of electron flow and proton transport were determined by fitting the respective experimental and simulated kinetic curves. In particular, effective rate constant for PQH_2 oxidation by the Cyt b_6f complex was derived by comparing calculated and experimental plots for the rates of the post-illumination reduction of P^+_{700} at different pH_{in} ("Appendix 3", Fig. 13).

Effective rate constants of the transmembrane proton transport coupled to ATP synthesis and passive leak of protons through the thylakoid membrane were determined by the comparison of calculated and experimental data on the light-induced acidification of the thylakoid lumen (for details, see "Appendix 2"; Dubinskii and Tikhonov 1995). The values of the rate constants, which characterize different stages of the electron transfer along the ETC, from the water-splitting complex of PSII to PSI acceptors, were chosen on the basis of the literature data on the kinetics of partial reactions of electron transport in different segments of the chloroplast ETC as described above. The characteristic times of electron transfer reactions are given in Table 1.

Appendix 2: proton transport and ATP synthesis in the model

There are indications that the proton conductivity of a lipid bilayer is determined mainly by the presence of acidic groups in the membrane (Deamer 1987; Gutknecht 1987; Nagle 1987). In this work, the equations for the active (J_{ATP}) and passive (J_{pass}) fluxes of protons were derived from a simple model based on the assumption that the processes of the transmembrane transfer of protons occur through the acidic groups bound either to the ATP synthase or buried inside the thylakoid membrane, respectively (Dubinskii and Tikhonov 1995). According to the model considered in our work, the proton transfer through the CF_o segment of the ATP synthase includes stages of protonation and deprotonation of carboxyl groups of the c_m-ring: $–COO^- + H^+_{in} \rightarrow –COOH \rightarrow –COO^- + H^+_{out}$. Concerning the passive *trans*-thylakoid transport of H^+ ions, we assume that the proton first binds to the intramembrane proton-accepting group and then dissociates into the stroma. The efficient rate constants of the proton exchange with the proton-accepting group are indicated in Fig. 3b. The rate constants of the direct and reverse reactions are related by the ratio $k^{in}_1/k^{in}_{-1} = K_{M1}$ and $k^{out}_2/k^{out}_{-2} = K_{M2}$, where K_{M1} and K_{M2} are the effective constants of the proton equilibrium for the buffer group $–COO^-$ and hydrogen ions inside and outside of the thylakoid, respectively. It is reasonable to assume that, for the proton-accepting groups $–COO^-$ fixed in the membrane and involved in the passive transfer of protons across the membrane, the equality $K_{M1} = K_{M2} \equiv K_M$ must be true. Fitting of the rate constant parameters related to proton transfer through the membrane acidic groups has been performed by means of the comparison of calculated and experimental data on the light-induced uptake of protons by the chloroplasts (Dubinskii and Tikhonov 1995). For the ΔpH-driven flux of protons through the ATP synthase, J_{ATP}, coupled to ATP synthesis, we used the following relationship:

$$J_{ATP} = k_{ATP}(T) \cdot \left([ADN]_0 - [ATP]\right) \cdot \frac{[H^+_{out}] \cdot [10^{\Delta pH} - 1]}{\alpha + [H^+_{out}] \cdot [10^{\Delta pH} + \beta]}, \quad \text{(A8)}$$

where $\Delta pH = pH_{out} - pH_{in}$ is the driving force for the operation of the ATP synthase (for details, see Tikhonov and Vershubskii 2014). Coefficients α and β are the model parameters, the values of which are determined by pK_A of the acidic group –COO^- of the c_n-ring of the ATP synthase and the values of the efficient rate constants k_1 and k_2 characterizing proton transport to -COO^- from the lumen and stroma, respectively; $\alpha = 10^{-pK_A}(1 + \beta)$, $\beta = k_2^{out}/k_1^{in}$. In our calculations we used the model parameters $pK_A = 7.3$ and $\beta = 20$, which values have been chosen on the basis of our previous works (Vershubskii et al. 2011, 2017, 2018; Vershubskii and Tikhonov 2020). Formula (A8) provides a sigmoid dependence of the ATP synthesis rate versus the proton-motive force ΔpH (Fig. 3c), which is typical of experimental force–flux relationships in chloroplasts (Turina et al. 2016). Note that variations of the model parameters α and β influence markedly a threshold ΔpH_{th}, above which value the ATP synthase efficiently produces ATP. Numerical values of the model parameters, related to the *trans*-thylakoid proton transfer, were determined by fitting theoretical curves to relevant experimental dependences of the light-induced acidification of the lumen at different values of external pH_{out}. Fitting of the rate constants k_1^{in}, k_{-1}^{in}, k_2^{in}, and k_{-2}^{in} was performed earlier (Dubinskii and Tikhonov 1995).

The model parameter k_{H^+}, which stands in the right side of Eq. A7, determines the passive efflux of protons (J_{pass}) from the lumen to the outer space: $J_{pass} = k_{H^+}(T) \cdot ([H^+_{in}] - [H^+_{out}])$. The $k_{H^+}(T)$ values were chosen by means of fitting calculated values of J_{pass} to experimentally measured proton fluxes determined for chloroplasts in the metabolic state 4 (compare experimental and theoretical data in Fig. 4c).

It is well-known fact that the ATP synthase activity is controlled by the redox status of chloroplasts. The light-induced activation of the ATP synthase is associated with the reduction of the thiol groups in the subunit γ, rotating together with the c_n-ring (Bakker-Grunwald and van Dam 1974; Bald et al. 2001). It is conceivable that the reduction of these groups may be mediated through the pigments found in the central cavity of the c_{14}-rotor (Varco-Merth et al. 2008; Vlasov et al. 2019). In the current work, however, we ignored this effect, because we compared experimental and theoretical data on the initial phase of the light-induced ATP synthesis (during 10-s illumination), when the linear growth of ATP concentration was not affected by the light-induced modulation of the chloroplast ATP synthase. According to our previous measurements, the light-induced activation of the ATP synthase was observed after 2 min of chloroplast illumination in the presence of methylviologen (data not shown).

Appendix 3: materials and experimental methods

Plant material and preparation of chloroplasts

Class B chloroplasts were isolated from greenhouse bean leaves (*Vicia faba*, 2–3 weak old) as described by Tikhonov et al. (1981). Chloroplasts were suspended at a final concentration of 2–3 mg chlorophyll/ml in the medium containing 0.2 M sucrose, 2 mM $MgCI_2$, and 10 mM Tricine-NaOH buffer (pH between 6.5 and 9.5) or Mes-HCl buffer (pH between 4.5 and 6.5). For measurements of chloroplast activity at different pH of the chloroplast suspension, we also used the medium which contained 0.2 M sucrose, 2 mM $MgC1_2$, 10 mM phosphate-citrate buffer, and 4 mM Mg-ADP. 20 μM methylviologen was used as a mediator of electron transfer from PSI to molecular oxygen. The pH value of the suspending medium was checked with a Radiometer glass electrode GK2321C.

In this work, we refer to experimental results described in earlier works of our group (Tikhonov et al. 1980, 1981, 1983, 1984; Timoshin et al. 1984; Kukushkin and Tikhonov 1988; Tikhonov and Subczynski 2005). The batches of chloroplasts used in these works were isolated from bean leaves of different harvests, including plants grown under variable experimental conditions (different seasons and concomitant changes in environmental conditions). In general, plants were cultivated at growth temperatures in the range 18–32 °C, depending on the season. We found that variability in the plant cultivation conditions could cause somewhat different temperature dependences of photosynthetic processes in isolated bean chloroplasts (compare, for example, panels c, d, and e in Fig. 9). Variability of this kind proved useful for analyzing the structure–function relationships in chloroplasts. In particular, statistically significant coincidence of the peculiar temperatures of the "structural" (membrane fluidity) and "functional" (ATP synthesis) characteristics was observed for each individual batch of chloroplasts (Fig. 9). Inflexion points in temperature dependences of the plots of "structural" and "functional" parameters coincided with a sufficiently high precision (±1 °C). In the meantime, the harvest-depending scattering of these peculiar points was more significant (for example, in the range 25–33 °C, Fig. 9). This observation allowed us to suggest that the temperature dependences of electron and proton transport processes were controlled by the physical state of thylakoid membranes.

EPR measurements of PSII activity and the intersystem electron transfer

The redox transients of P_{700} were monitored by measuring the light-induced changes in the amplitude of the EPR signal from P^+_{700} (Tikhonov et al. 1980, 1981; Tikhonov 2015). The EPR measurements of P^+_{700} were performed with a Varian EPR spectrometer (model E-4) at 4 G modulation amplitude and 10 mW microwave power. Far-red background illumination (interference filter SIF707, Karl Zeiss Jena; λ_{max} = 707 nm, $\Delta\lambda_{1/2}$ = 5 nm) was applied to provide the re-oxidation of the ETC between PSII and PSI. The intensity of this light, provided by a 150 W incandescent lamp equipped with a water filter and focusing lens, was adjusted to reach maximal level of P_{700} oxidation. A similar light source without the interference filter (white light) was used for efficient excitation of both photosystems. Two kinds of white light pulses of were used to test PSII activity: (i) short flashes ($\tau_{1/2}$ = 7 µs) of saturating intensity, and (ii) long flashes ($\tau_{1/2}$ = 750 µs) were applied for multiple operation of P_{680}. The energy released in the discharge circuit was 10 and 100 J, respectively (Tikhonov et al. 1980).

Figure 12a shows a simplified diagram illustrating electron transfer from PSII and O_2, the terminal acceptor of electrons donated by PSI. Illumination of chloroplasts by the far-red (or white) light induces generation of the EPR signal from P^+_{700} shown in Fig. 12b. After sudden shutdown of white light (WL), P^+_{700} rapidly reduces due to electrons

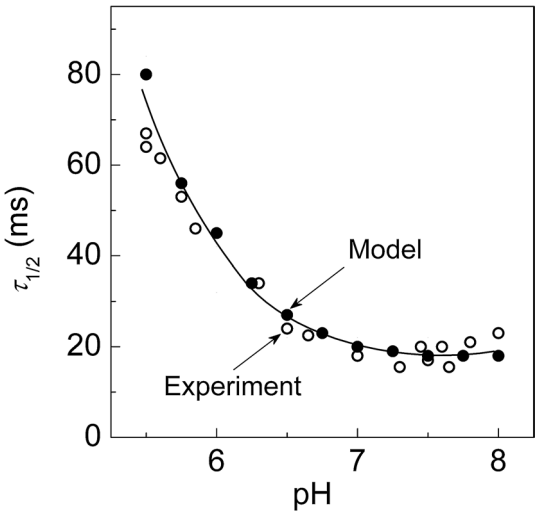

Fig. 13 Experimental and theoretical dependencies of the half-time of P^+_{700} reduction after switching off the white light on the intra-thylakoid pH_{in}. *Open symbols*, experimental data; *filled symbols*, calculated data. Experimental points were obtained for the suspension of uncoupled chloroplasts (on the basis of results published in Tikhonov et al. 1984)

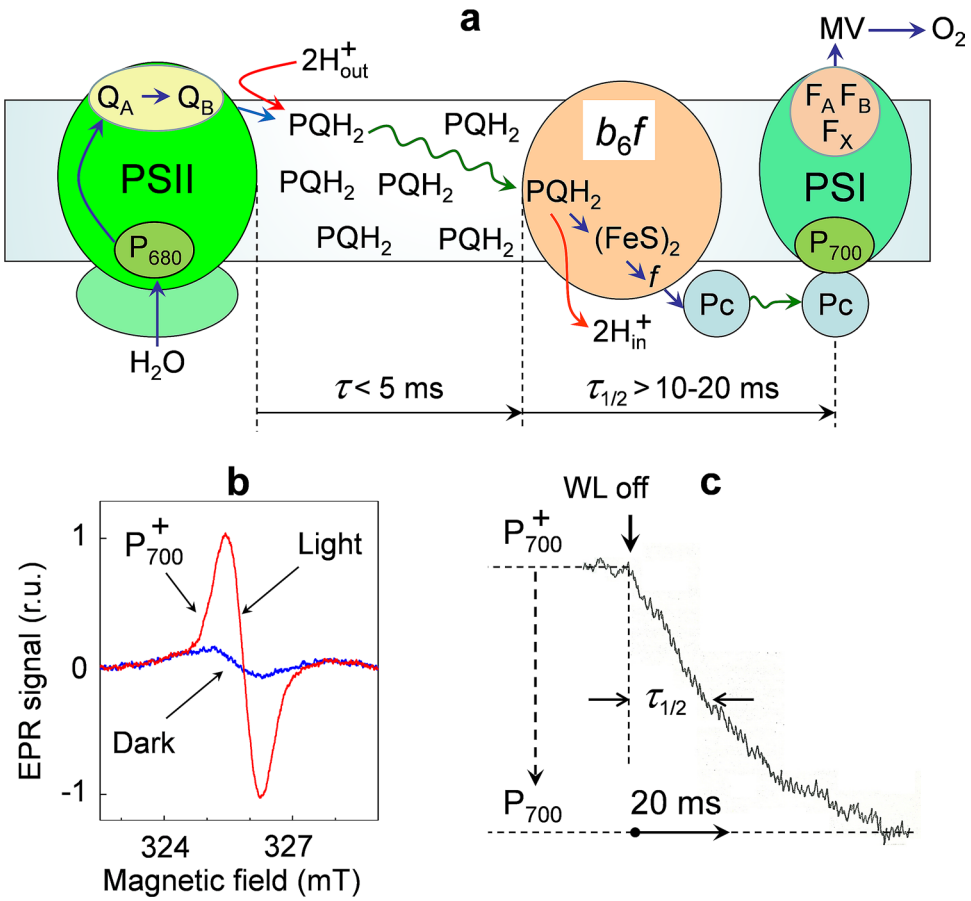

Fig. 12 Simplified diagram illustrating electron transfer from PSII and O_2, the terminal acceptor of electrons donated by PSI (panel **a**); EPR signals of bean chloroplasts in the dark and during illumination with the far-red light, λ_{max} = 707 nm, as indicated (panel **b**); the post-illumination kinetics of P^+_{700} reduction in bean chloroplasts pre-illuminated by continuous white light (panel **c**) Modified figures adopted from (Tikhonov et al. 1984)

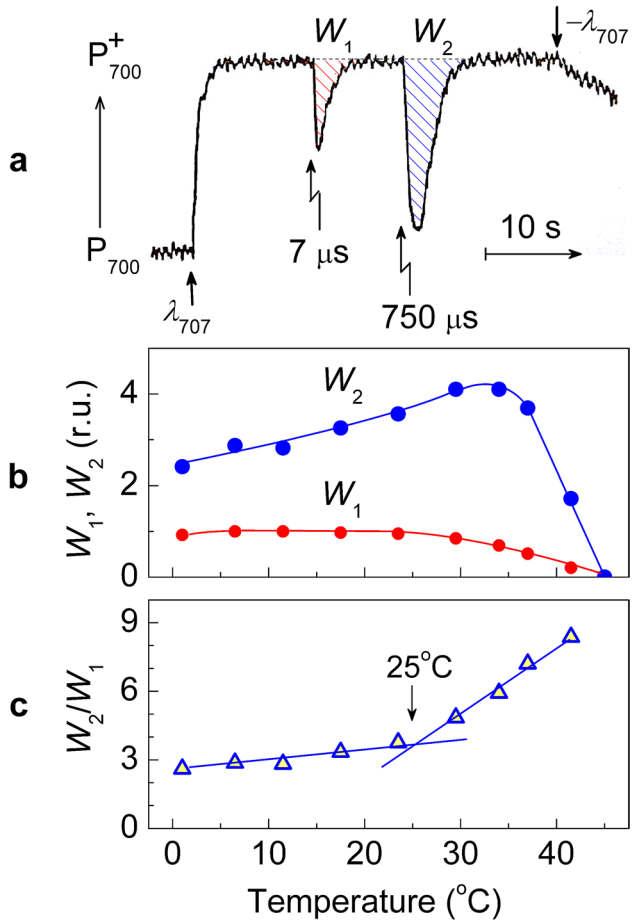

Fig. 14 **a** The light-induced redox transients of P_{700} in bean chloroplasts induced by the far-red light (λ_{707}) and pulses of white light of different durations. Parameters W_1 and W_2 are proportional to the numbers of electrons injected into intersystem electron transport chain (for other details see text and Tikhonov et al. 1980). **b** Temperature dependences of parameters W_1 and W_2 shown in the panel **a**. **c** Temperature dependence of the ratio $f = W_2(T)/W_1(T)$, which determines a number of electrons donated by PSII during the action of the long flash

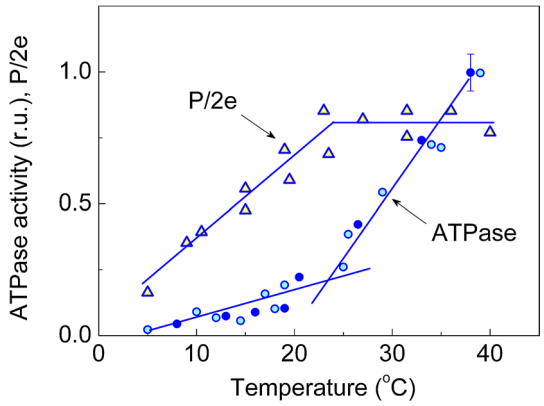

Fig. 15 Temperature dependences of parameter P/2e, which denotes the ratio between the rates of photophosphorylation (ADP + P_i → ATP) and pseudocyclic electron flow and ATPase activity of bean chloroplasts (closed and open symbols were obtained on different batches of chloroplasts) Modified figures after (Timoshin et al. 1984)

donated by reduced PQH_2 molecules (Fig. 12c). The half-time of P^+_{700} decay (parameter $\tau_{1/2}$) characterizes the rate of electron transfer from PQH_2 to P^+_{700}.

Figure 13 shows experimental and theoretical dependencies of the half-time of P^+_{700} reduction after switching off the white light on the intra-thylakoid pH_{in}. Open symbols, experimental data; filled symbols, calculated data. Experimental points were obtained for the suspension of uncoupled chloroplasts (on the basis of results published by Tikhonov et al. (1980)).

Figure 14a shows the time-course of P_{700} redox changes in aerated suspension of bean chloroplasts. Illumination of chloroplasts by the far-red light (λ_{707}), absorbed predominantly by PSI, induced oxidation of P_{700}. Application of a short saturating pulse ($\tau_{1/2}$ = 7 μs) induced the reduction of P^+_{700} due to the injection of electrons from PSII to the intersystem ETC. The reduction of P^+_{700} is followed by the re-oxidation of P_{700} due to the action of the continuous far-red light. The area W_1 over the kinetic curve can serve as a measure of PSII photochemical activity: in response to a short flash, each PSII donates one electron (on an average). In this case, the Mn_4Ca cluster is oxidized by one electron and one electron is donated to the intersystem ETC (Cardona et al. 2012). After the action of a prolonged flash ($\tau_{1/2}$ = 750 μs), the area over the kinetic curve (parameter W_2) increases. This occurs due to a multiple charge separations in PSII and donation of several electrons to the PQ pool (Tikhonov and Vershubskii 2017). Figure 14b shows the temperature dependences of parameters W_1 and W_2. The ratio $f = W_2/W_1$ is determined by the rate of electron transfer from PSII to the PQ pool (Fig. 14c). The temperature of a sample was regulated with the Varian temperature controller.

Potentiometry methods of assaying the chloroplasts activity

The rate of pseudocyclic electron flow J_{Fd-O2} (H_2O → PSII → PSI → MV → O_2; the so-called "water-water" cycle; Asada 1999) was determined by measuring the O_2 uptake ($O_2 + e^- \rightarrow O_2^{\bullet-}$) in an aerated suspension of chloroplasts, using a laboratory-made Clark-type electrode. In this case, the superoxide and catalase activities of chloroplasts were inhibited by the addition of small amounts of NaN_3 as described earlier (Timoshin et al. 1984).

The rate of ATP formation (V_{ATP}) was routinely measured by the potentiometry method (Nishimura et al. 1962; Timoshin et al. 1984). All controls including that of adenylate kinase activity were properly made. Adequacy of potentiometric measurements of photophosphorylation

($ADP + P_i \rightarrow ATP + H_2O$) was verified independently by the use of enzymatic (Malenkova et al. 1982) and modified luciferin-luciferase (Ataullakhanov and Pichugin 1981) methods. The rate of ATP hydrolysis was also determined by measuring changes in the ^{31}P NMR spectra of ATP, ADP, and P_i in bean chloroplast suspension according to (Ogawa et al. 1980). Results of this study, performed together with professor E.K. Ruuge, will be published elsewhere.

Having measured, under the same experimental conditions, the rates of ATP synthesis (V_{ATP}) and electron transport (J_{Fd-O2}), we could determine the ratio V_{ATP}/J_{Fd-O2}, which characterizes the efficiency of coupling of electron transport and ATP synthesis (often termed as the so-called ratio "P/2e"; Ivanov 1993). Figure 15 reproduces the temperature dependence of the ratio P/2e that was determined earlier in our work (Timoshin et al. 1984). As one can see, the ratio P/2e increases with temperature, reaching a plateau at temperatures above 25 °C.

Measurements of ΔpH generation

Transmembrane pH difference (ΔpH) across the thylakoid membrane was measured by three independent methods based on the use of the EPR technique: (1) the determination of the pH_{in}-dependent rate of the intersystem electron transfer from the kinetics of the post-illumination reduction of P_{700}^+ (Tikhonov et al. 1981, 1984), (2) the use of pH-sensitive water-soluble spin probes located in the thylakoid lumen (Tikhonov et al. 2008; Tikhonov 2017; Vershubskii et al. 2017), and (3) the determination of ΔpH in chloroplasts from the partitioning of a water-soluble spin label tempamine (Trubitsin and Tikhonov 2003; Tikhonov 2017). We used experimental data on ΔpH measurements in bean chloroplasts in order to perform the final fitting of the model parameters (see, for example, Vershubskii and Tikhonov 2020).

Spin-labeling study of *thermo*-induced structural changes in thylakoid membranes

Thermo-induced changes in the lipid domains of the thylakoid membranes were studied with the lipid-soluble spin probes, paramagnetic derivatives of stearic acid, 5-SASL (Fig. 9b), as described in Tikhonov et al. (1980, 1983), Timoshin et al. (1984), Lutova and Tikhonov (1988), Ligeza et al. (1998), and Tikhonov and Subczynski (2005). A small aliquot (1% v/v) of 5-SASL dissolved in ethanol was added to chloroplast suspension. After 10-min incubation of thylakoids with the spin probe, the suspension of spin-labeled thylakoids was used for EPR measurements. The temperature of a sample placed into the cavity of a Varian (E-4) X-band EPR spectrometer was regulated with the Varian temperature controller, with precision up to ± 0.5 °C.

References

Agalarov R, Brettel K (2003) Temperature dependence of biphasic forward electron transfer from the phylloquinone(s) A_1 in photosystem I: only the slower phase is activated. Biochim Biophys Acta 1604:7–12

Albertsson PE (2001) A quantitative model of the domain structure of the photosynthetic membrane. Trends Plant Sci 6:349–354

Allakhverdiev SI, Kreslavski VD, Klimov VV, Los DA, Carpentier R, Mohanty P (2008) Heat stress: an overview of molecular responses in photosynthesis. Photosynth Res 98:541–550

Allen DJ, Ort DR (2001) Impact of chilling temperatures on photosynthesis in warm climate plants. Trends Plant Sci 6:36–42

Aloia RA, Boggs JM (eds) (1985) Membrane fluidity in biology. Academic Press, New York, pp 147–208

Anderson JM (1982) Distribution of the cytochromes of spinach chloroplasts between the appressed membranes of grana stacks and stroma-exposed thylakoid regions. FEBS Lett 138:62–66

Ariga T, Muneyuki E, Yoshida M (2007) F1-ATPase rotates by an asymmetric, sequential mechanism using all three catalytic subunits. Nat Struct Mol Biol 14:841–846

Arnold A, Nikoloski Z (2011) A quantitative comparison of Calvin-Benson cycle models. Trends Plant Sci 16:676–683

Asada K (1999) The water–water cycle in chloroplasts: scavenging of active oxygens and dissipation of excess photons. Ann Rev Plant Physiol Plant Mol Biol 50:601–639

Ataullakhanov FI, Pichugin AV (1981) Modification of luciferin-luciferase method for ATP assay in erythrocytes. Biophysics (USSR) 26:81–86

Badger MR, Von Caemmerer S, Ruuska S, Nakano H (2000) Electron flow to oxygen in higher plants and algae: rates and control of direct photoreduction (Mehler reaction) and rubisco oxygenase. Philos Trans R Soc London 355:1433–1446

Bakker-Grunwald T, van Dam K (1974) On the mechanism of activation of the ATPase in chloroplasts. Biochim Biophys Acta 347:290–298

Bald D, Noji H, Yoshida M, Hirono-Hara Y, Hisabori T (2001) Redox regulation of the rotation of F_1-ATP synthase. J Biol Chem 276:39505–39507

Baniulis D, Yamashita E, Zhang H, Hasan SS, Cramer WA (2008) Structure–function of the cytochrome b_6f complex. Photochem Photobiol 84:1349–1358

Barber J, Ford RC, Mitchell RA, Millner PA (1984) Chloroplast thylakoid membrane fluidity and its sensitivity to temperature. Planta 161:375–380

Bendall DS, Manasse RS (1995) Cyclic photophosphorylation and electron transport. Biochim Biophys Acta 1229:23–38

Benkov MA, Yatsenko AM, Tikhonov AN (2019) Light acclimation of shade-tolerant and sun-resistant *Tradescantia* species: photochemical activity of PSII and its sensitivity to heat treatment. Photosynth Res 139:203–214

Benson BB, Krause Jr D (1984) The concentration and isotopic fractionation of oxygen dissolved in freshwater and seawater in equilibrium with the atmosphere. Limnol Oceanogr 29:620–632

Berliner LJ (ed) (1976) Spin labeling: theory and applications. Academic Press, New York-London

Berry J, Björkman O (1980) Photosynthetic response and adaptation to temperature in higher plants. Annu Rev Plant Physiol 31:491–543

Boardman NK (1977) Comparative photosynthesis of sun and shade plants. Ann Rev Plant Physiol 28:335–377

Boudiere L, Michaud M, Petroutsos D, Rebeille F, Falconet D, Bastien O, Roy S, Finazzi G, Rolland N, Jouhet J et al (2014) Glycerolipids in photosynthesis: composition, synthesis and trafficking. Biochim Biophys Acta 1837:470–480

Boyer PD (1997) The ATP synthase—a splendid molecular machine. Annu Rev Biochem 66:717–749

Brandt U (1996) Bifurcated ubihydroquinone oxidation in the cytochrome bc_1 complex by proton-gated charge transfer. FEBS Lett 387:1–6

Brettel K (1997) Electron transfer and arrangement of the redox cofactors in photosystem I. Biochim Biophys Acta 1318:322–373

Brettel K, Leibl W (2001) Electron transfer in photosystem I. Biochim Biophys Acta 1507:100–114

Cardona T, Sedoud A, Cox N, Rutherford AW (2012) Charge separation in photosystem II: a comparative and evolutionary overview. Biochim Biophys Acta 1817:26–43

Chance B, Williams GR (1956) The respiratory chain and oxidative phosphorylation. Adv Enzymol 17:65–134

Cherepanov DA, Milanovsky GE, Petrova AA, Tikhonov AN, Semenov AYu (2017) Electron transfer through the acceptor side of Photosystem I: interaction with exogenous acceptors and molecular oxygen. Biochemistry (Moscow) 82:1249–1268

Clever HL, Battino R, Miyamoto H, Yampolski Y, Young CL (2014) IUPAC-NIST Solubility Data Series. 103. Oxygen and Ozone in Water, Aqueous Solutions, and Organic Liquids (Supplement to Solubility Data Series Volume 7). J Phys Chem Ref Data 43(3)

Cramer WA, Hasan SS (2016) Structure-function of the cytochrome b_6f lipoprotein complex. In cytochrome complexes: evolution, structures, energy transduction, and signaling. Adv Photosynth Respiration 41:177–207

Cramer WA, Zhang H, Yan J, Kurisu G, Smith JL (2006) Transmembrane traffic in the Cytochrome b_6f complex. Ann Rev Biochem 75:769–790

Cramer WA, Hasan SS, Yamashita E (2011) The Q cycle of cytochrome *bc* complexes: a structure perspective. Biochim Biophys Acta 1807:788–802

Crofts AR (2004) Proton-coupled electron transfer at the Q_o-site of the bc_1 complex controls the rate of ubihydroquinone oxidation. Biochim Biophys Acta 1655:77–92

Crofts AR, Wang Z (1989) How rapid are the internal reactions of the ubiquinol:cytochrome c_2 oxidoreductase? Photosynth Res 22:69–87

Crofts AR, Guergova-Kuras M, Kuras R, Ugulava N, Li J, Hong S (2000) Proton-co;upled electron transfer at the Q_o-site: what type of mechanism can account for the high activation barrier? Biochim Biophys Acta 1459:456–466

Crofts AR, Hong S, Wilson C, Burton R, Victoria D, Harrison C, Schulten K (2013) The mechanism of ubihydroquinone oxidation at the Q_o-site of the cytochrome bc_1 complex. Biochim Biophys Acta 1827:1362–1377

Dau H, Haumann M (2008) The manganese complex of photosystem II in its reaction cycle—basic framework and possible realization at the atomic level. Coord Chem Rev 252:273–295

Davis GA, Rutherford AW, Kramer DM (2017) Hacking the thylakoid proton motive force for improved photosynthesis: modulating ion flux rates that control proton motive force partitioning into $\Delta\psi$ and ΔpH. Philos Trans R Soc B 372:20160381

de Wijn R, van Gorkom HJ (2001) Kinetics of electron transfer from Q_A to Q_B in photosystem II. Biochemistry 40:11912–11922

Deamer DW (1987) Proton permeation of lipid bilayers. J Bioenerg Biomembr 19:457–479

Dekker JP, Boekema EJ (2005) Supermolecular organization of the thylakoid membrane proteins in green plants. Biochim Biophys Acta 1706:12–39

Demmig-Adams B, Cohu CM, Muller O et al (2012) Modulation of photosynthetic energy conversion efficiency in nature: from seconds to seasons. Photosynth Res 113:75–88

Díaz-Quintana A, Leibl W, Bottin H, Sétif P (1998) Electron transfer in photosystem I reaction centers follows a linear pathway in which iron–sulfur cluster FB is the immediate electron donor to soluble ferredoxin. BioChemistry 37:3429–3439

Diez M, Zimmermann B, Borsch M, Konig M, Schweinberger E, Steigmiller S, ReuterR Felekyan S, Kudryavtsev V, Seidel CA, Graber P (2004) Proton-powered subunit rotation in single membrane-bound F0F1-ATP synthase. Nat Struct Mol Biol 11:135–141

Dubinskii AYu, Tikhonov AN (1995) Mathematical simulation of the light-induced uptake of protons by chloroplasts upon various mechanisms of proton leak through the thylakoid membrane. Biophysics 40:365–371

Dubinskii AYu, Tikhonov AN (1997) Mathematical model of thylakoid as the distributed heterogeneous system of electron and proton transport. Biophysics 42:644–660

Edwards G, Walker D (1983) C3, C4: mechanisms, and cellular and environmental regulation, of photosynthesis. Univ of California Press, Berkeley

Fillingame RH, Jiang W, Dmitriev OY (2000) Coupling H^+ transport to rotary catalysis in F-type ATP synthases: structure and organization of the transmembrane rotary motor. J Exp Biol 203:9–17

Ford RC, Barber J (1983) Incorporation of sterol into chloroplast thylakoid membranes and its effect on fluidity and function. Planta 158:35–41

Ford RC, Chapman DJ, Barber J, Pedersen JZ, Cox RP (1982) Fluorescence polarization and spin-label studies of the fluidity of stromal and granal chloroplast membranes. Biochim Biophys Acta 681:145–151

Foyer CH, Neukermans J, Queval G, Noctor G, Harbinson J (2012) Photosynthetic control of electron transport and the regulation of gene expression. J Exp Bot 63:637–1661

Gong X-S, Chung S, Fernandez-Velasco JG (2001) Electron transfer and stability of the cytochrome b_6f complex in a small domain deletion mutant of cytochrome *f*. J Biol Chem 276:24365–24371

Gounaris K, Brain APR, Quinn PJ, Williams WP (1984) Structural reorganization of chloroplast thylakoid membranes in response to heat-stress. Biochim Biophys Acta 766:198–208

Griffith OH, Jost PC (1976) Lipid spin labels in biological membranes. Spin labeling: theory and applications. Academic Press, New York, pp 456–524

Gutknecht J (1987) Weak electrolyte transport across biological membranes. General principles. J Bioenerg Biomembr 19:427–455

Haehnel W (1973) Electron transport between plastoquinone and chlorophyll a_I. Biochim Biophys Acta 305:618–631

Haehnel W (1976) The reduction kinetics of chlorophyll a_1 as an indicator of for proton uptake between the light reactions in chloroplasts. Biochim Biophys Acta 440:506–521

Haehnel W (1984) Photosynthetic electron transport in higher plants. Annu Rev Plant Physiol 35:659–693

Hasan SS, Cramer WA (2012) On rate limitation of electron transfer in the photosynthetic b_6f complex. Phys Chem Chem Phys 14:13856–13860

Hasan SS, Cramer WA (2014) Internal lipid architecture of the heterooligomeric cytochrome b_6f complex. Structure 22:1–8

Hasan SS, Yamashita E, Baniulis D, Cramer WA (2013a) Quinone-dependent proton transfer pathways in the photosynthetic cytochrome b_6f complex. Proc Natl Acad Sci USA 110:4293–4302

Hasan SS, Stofleth JT, Yamashita E, Cramer WA (2013b) Lipid-induced conformational changes within the cytochrome b_6f complex of oxygenic photosynthesis. Biochemistry 52:2649–2654

Heise K-P, Harnischfeger G (1978) Correlation between photosynthesis and plant lipid composition. Z Naturforsch 33:537–546

Hirano M, Satoh K, Katoh S (1981) The effect on photosynthetic electron transport of temperature-dependent changes in the fluidity of the thylakoid membrane in a thermophilic blue-green alga. Biochim Biophys Acta 635:476–487

Hong SJ, Ugulava N, Guergova-Kuras M, Crofts AR (1999) The energy landscape for ubihydroquinone oxidation at the Q_o-site of the bc_1 complex in *Rhodobacter sphaeroides*. J Biol Chem 274:33931–33944

Hope AB (2000) Electron transfers amongst cytochrome *f*, plastocyanin and photosystem I: kinetics and mechanisms. Biochim Biophys Acta 1456:5–26

Horton P (2012) Optimization of light harvesting and photoprotection: molecular mechanisms and physiological consequences. Phil Trans R Soc B 367:3455–3465

Hu S, Ding Y, Zhu C (2020) Sensitivity and responses of chloroplasts to heat stress in plants. Front Plant Sci 11:375. https://doi.org/10.3389/fpls.2020.00375

Igamberdiev AU (2011) Computational models of photosynthesis. BioSystems 103:113–314

Inout H (1978) Break points in Arrhenius plots of the Hill reaction of spinach chloroplast fragments in the temperature range from -25 to 25°C. Plant Cell Physiol 19:355–363

Ivanov BN (1993) Stoichiometry of proton uptake by thylakoids during electron transport in chloroplasts. In: Abrol YP, Mohanty P, Govindjee G (eds) Photosynthesis: Photoreactions to Plant Productivity. Springer, Dordrecht, pp 108–128

Johnson MP, Ruban AV (2014) Rethinking the existence of a steady-state $\Delta\psi$ component of the proton motive force across plant thylakoid membranes. Photosynth Res 119:233–242

Junge W, Nelson N (2015) ATP synthase. Annu Rev Biochem 83:631–657

Junge W, Lill H, Engelbrecht S (1997) ATP synthase: an electrochemical transducer with rotatory mechanics. Trends Biochem Sci 22:420–423

Karavaev VA, Kukushkin AK (1993) Theoretical model of the light and dark stages of photosynthesis: the regulation problem. Biophysics 38:958–975

Kern J, Zouni A, Guskov A, Krauβ N (2009) Lipid in the structure of photosystem I, photosystem II and the cytochrome b_6f complex. In: Wada H, Murata N (eds) Lipids in Photosynthesis: Essential and Regulatory Functions. Springer, Dordrecht, pp 203–242

Kirchhoff H (2008) Significance of protein crowding, order and mobility for photosynthetic membrane functions. Biochem Soc Trans 36:967–970

Kirchhoff H (2014) Diffusion of molecules and macromolecules in thylakoid membranes. Biochim Biophys Acta 1837:495–502

Kirchhoff H, Horstmann S, Weis E (2000) Control of the photosynthetic electron transport by PQ diffusion microdomains in thylakoids of higher plants. Biochim Biophys Acta 1459:148–168

Kirchhoff H, Hall C, Wood M, Herbstová M, Tsabari O, Nevo R, Charuvi D, Shimoni E, Reich Z (2011) Dynamic control of protein diffusion within the granal thylakoid lumen. Proc Natl Acad Sci USA 108:20248–20253

Kraayenhof R, Katan MB, Grunwald T (1971) The effect of temperature on energy-linked functions in chloroplasts. FEBS Lett 19:5–10

Kramer DM, Sacksteder CA, Cruz JA (1999) How acidic is the lumen? Photosynth Res 60:151–163

Kukushkin AK, Tikhonov AN (1988) Lectures on Biophysics of Photosynthesis in Higher Plants. Moscow University Press, Moscow **(in Russian)**

Kumamoto J, Raison JK, Lyons JM (1971) Temperature "breaks" in Arrhenius plots: a thermodynamic consequence of a phase change. J Theor Biol 31:47–51

Kuvykin IV, Vershubskii AV, Ptushenko VV, Tikhonov AN (2008) Oxygen as an alternative electron acceptor in the photosynthetic electron transport chain of C3 plants. Biochemistry (Moscow) 73:1063–1075

Laisk A, Nedbal N, Govindjee (eds) (2009) Photosynthesis in silico. Understanding complexity from molecules to ecosystems. Springer, Dordrecht

Lazár D, Schansker G (2009) Models of chlorophyll *a* fluorescence transients. In: Laisk A, Nedbal L, Govindjee S (eds) Photosynthesis in silico: understanding complexity from molecules to ecosystems. Advances in photosynthesis and respiration, vol 29. Springer, Dordrecht, pp 85–123

Lee AJ (1977) Lipid phase transitions and phase diagrams. I. Lipid phase transitions. Biochim Biophys Acta 472:237–281

Li Z, Wakao S, Fischer BB, Niyogi KK (2009) Sensing and responding to excess light. Annu Rev Plant Biol 60:239–260

Ligeza A, Tikhonov AN, Hyde JS, Subczynski WK (1998) Oxygen permeability of thylakoid membranes: electron paramagnetic resonance spin labeling study. Biochim Biophys Acta 1365:453–463

Link TA (1997) The role of the "Rieske" iron sulfur protein in the hydroquinone oxidation (Q_p) site of the cytochrome bc_1 complex: the "proton-gated affinity change" mechanism. FEBS Lett 412:257–264

Los DA, Murata N (2004) Membrane fluidity and its role in the perception of environmental signals. Biochim Biophys Acta 1666:142–157

Los DA, Mironov KS, Allakhverdiev SI (2013) Regulatory role of membrane fluidity in gene expression and physiological functions. Photosynth Res 116:489–509

Lubitz W, Chrysina M, Cox N (2019) Water oxidation in photosystem II. Photosynth Res 142:105–125

Lutova MI, Tikhonov AN (1983) Aftereffect of high temperature on photosynthesis and electron transport in wheat leaves. Biophysics 28:284–287

Lutova MI, Tikhonov AN (1988) Comparative study of temperature effects on the mobility of lipid- soluble spin label in thylakoid membranes of melon and cucumber chloroplasts. Biophysics 33:460–464

Luzikov VN, Novikova LA, Tikhonov AN, Zubatov AS (1983) Correlation between the rate of proteolysis of mitochondrial translation products and fluidity of the mitochondrial inner membrane of *Saccharomices cervisiae*. Biochem J 214:785–794

Luzikov VN, Novikova LA, Zubatov AS, Tikhonov AN (1984) Physical state of the mitochondrial inner membrane as a factor controlling the proteolysis of mitochondrial translational products in yeasts. Biochim Biophys Acta 775:22–30

Maksimov EG, Mironov KS, Trofimova MS, Nechaeva NL, Todorenko DA, Klementiev KE, Tsoraev GV, Tyutyaev EV, Zorina AA, Feduraev PV, Allakhverdiev SI, Paschenko VZ, Los DA (2017) Membrane fluidity controls redox-regulated cold stress responses in cyanobacteria. Photosynth Res 133:215–223

Malenkova IV, Kuprin SP, Davidov RM, Blumenfeld LA (1982) pH-jump-induced ADP phosphorylation in mitochondria. Biochim Biophys Acts 682:179–183

Mamedov M, Govindjee Nadtochenko V, Semenov A (2015) Primary electron transfer processes in photosynthetic reaction centers from oxygenic organisms. Photosynth Res 125:51–63

Margolis LB, Tikhonov AN, Vasilieva EYu (1980) Platelet adhesion to fluid and solid phospholipid membranes. Cell 19:189–194

McConnell HM (1976) Molecular motion in biological membranes. Spin labeling: theory and applications. Academic Press, New York, pp 525–561

Melnichenko NA, Koltunov AM, Vyskrebentsev AS, Bazhanov AV (2008) The temperature dependence of the solubility of oxygen in sea water according to the pulsed NMR data. Russ J Phys Chem 82:746–752

Meyer B, Schlodder E, Dekker JP, Witt HT (1989) O_2 evolution and Chl a_{II}^+ (P-680$^+$) nanosecond reduction kinetics in single flashes as a function of pH. Biochim Biophys Acta 974:36–43

Milanovsky GE, Petrova AA, Cherepanov DA, Semenov AY (2017) Kinetic modeling of electron transfer reactions in photosystem I complexes of various structures with substituted quinone acceptors. Photosynth Res 133:185–199

Mitchell P (1976) Possible molecular mechanisms of the protonmotive function of cytochrome systems. J Theor Biol 62:327–367

Mizusawa N, Wada H (2012) The role of lipids in photosystem II. Biochim Biophys Acta 1817:194–208

Möbius K, Savitsky A (2009) High-field EPR spectroscopy on proteins and their model systems: characterization of transient paramagnetic states. RSC Publishing, London

Moon BY, Higashi S, Gombos Z, Murata N (1995) Unsaturation of the membrane lipids of chloroplasts stabilizes the photosynthetic machinery against low-temperature photoinhibition in transgenic tobacco plants. Proc Natl Acad Sci USA 92:6219–6223

Morales A, Yin X, Harbinson J, Driever SM, Molenaar J, Kramer DM, Struik P (2018) In silico analysis of the regulation of the photosynthetic electron transport chain in C3 plants. Plant Physiol 176:1247–1261

Moser CC, Keske JM, Warncke K, Farid RS, Dutton PL (1992) Nature of biological electron transfer. Nature 355:796–802

Murata N, Fork DC (1977) Temperature dependence of the light-induced spectral shift of carotenoids in *Cvanidium caldarium* and higher plant leaves. Evidence for an effect of the physical phase of chloroplast membrane lipids on the permeability of the membranes to ions. Biochim Biophys Acta 461:365–378

Nagle JF (1987) Theory of passive proton conductance in lipid bilayers. J Bioenerg Biomembr 19:413–426

Nelson N, Yocum CF (2006) Structure and function of photosystems I and II. Annu Rev Plant Biol 57:521–565

Nie GY, Baker NR (1991) Modifications to thylakoid composition during development of maize leaves at low growth temperatures. Plant Physiol 95:184–191

Nievola CC, Carvalho CP, Carvalho V, Rodrigues E (2017) Rapid responses of plants to temperature changes. Temperature 4:371–405

Nishimura M, Ito T, Chance B (1962) Studies on bacterial photophosphorylation III. A sensitive and rapid method of determination of photophosphorylation. Biochim Biophys Acta 59:177–182

Niu Y, Xiang Y (2018) An overview of biomembrane functions in plant responses to high-temperature stress. Front Plant Sci 9:915

Nolan WG (1980) Effect of temperature on electron transport activities of isolated chloroplasts. Plant Physiol 66:234–237

Nolan WG (1981) Effect of temperature on proton efflux from isolated chloroplast thylakoids. Plant Physiol 67:1259–1263

Nolan WG, Smillie RM (1976) Multi-temperature effects on Hill reaction activity of barley chloroplasts. Biochim Biophys Acta 440:461–475

Nolan WG, Smillie RM (1977) Temperature-induced changes in Hill activity of chloroplasts isolated from chilling-sensitive and chilling-resistant plants. Plant Physiol 59:1141–1145

Ogawa S, Shen C, Castillo CLA (1980) NMR study of the cross-membrane pH gradient induced by ATP hydrolysis in mitochondria. Biochim Biophys Acta 590:159–169

Ort DR, Baker NR (2002) A photoprotective role for O_2 as an alternative electron sink in photosynthesis? Curr Opin Plant Biol 5:193–198

Osyczka A, Moser CC, Dutton L (2005) Fixing the Q cycle. Trends Biochem Sci 30:176–182

Page CC, Moser CC, Chen X et al (1999) Natural engineering principles of electron tunnelling in biological oxidation-reduction. Nature 402:47–52

Quinn PJ, Williams WP (1978) Plant lipids and their role in membrane function. Progr Biophys Molec Biol 34:107–173

Razeghifard MR, Klughammer C, Pace RJ (1997) Electron paramagnetic resonance kinetic studies of the S states in spinach thylakoids. Biochemistry 36:86–92

Reeves SG, Hall DO, West J (1972) Correlation of the stoichiometry of photophosphorylation with the integrity of isolated spinach chloroplasts. In: Forti G, Avron M, Melandri A (eds) Photosynthesis, two centuries after its discovery by Joseph Priestley. Springer, Dordrecht

Rigoulet M, Leverve X, Fontaine E, Ouhabi R, Guérin B (1998) Quantitative analysis of some mechanisms affecting the yield of oxidative phosphorylation: dependence upon both fluxes and forces. Mol Cell Biochem 184:35–52

Riznichenko GY, Belyaeva NE, Kovalenko IB, Rubin AB (2009) Mathematical and computer modeling of primary photosynthetic processes. Biophys 54:10–22

Romanovsky YuM, Tikhonov AN (2010) Molecular energy transducers of the living cell. Proton ATP synthase: a rotating molecular motor. Phys Usp 53:893–914

Rubin A, Riznichenko G (2014) Mathematical biophysics. Series: biological and medical physics, biomedical engineering, XV

Sanderson DG, Anderson LB, Gross EL (1986) Determination of the redox potential and diffusion coefficient of the protein plastocyanin using optically transparent filar electrodes. Biochim Biophys Acts 852:269–278

Santabarbara S, Redding KE, Rappaport F (2009) Temperature dependence of the reduction of P_{700}^{+} by tightly bound plastocyanin *in vivo*. Biochemistry 48:10457–10466

Sarcina M, Murata N, Tobin MJ, Mullineaux CW (2003) Lipid diffusion in the thylakoid membranes of the cyanobacterium *Synechococcus* sp.: effect of fatty acid desaturation. FEBS Lett 553:295–298

Sawada S, Miyachi S (1974) Effects of growth temperature on photosynthetic carbon metabolism in green plants I. Photosynthetic activities of various plants acclimatized to varied temperatures. Plant Cell Physiol 15:111–120

Schneider AR, Geissler PL (2013) Coexistance of fluid and crystalline phases of proteins in photosynthetic membranes. Biophys J 105:1161–1170

Schuurmans JJ, Kraayenhof R (1983) Energy-regulated functional transitions of chloroplast ATPase. Photochem Photobiol 37:85–91

Seelert H, Poetsch A, Dencher NA, Engel A, Stahlberg H, Müller DJ (2000) Structural biology. Proton-powered turbine of a plant motor. Nature 405:418–419

Setif PQY, Bottin H (1994) Laser flash absorption spectroscopy study of ferredoxin reduction by Photosystem I in *Synechocystis* sp. PCC 6803: Evidence for submicrosecond and microsecond kinetics. Biochemistry 33:8495–8504

Shelaev IV, Gostev FE, Mamedov MD, Sarkisov OM, Nadtochenko VA, Shuvalov VA, Semenov AYu (2010) Femtosecond primary charge separation in photosystem I. Biochim Biophys Acta 1797:1410–1420

Shneyour A, Raison JK, Smillie RM (1973) The effect of temperature on the rate of photosynthetic electron transfer in chloroplasts of chilling-sensitive and chilling-resistant plants. Biochim Biophys Acta 292:152–161

Sigfridsson K (1998) Plastocyanin, an electron transfer protein. Photosynth Res 57:1–28

Siggel U (1976) The function of plastoquinone as electron and proton carrier in photosynthesis. Bioelectrochem Bioenerg 3:302–318

Staehelin LA (2003) Chloroplast structure: from chlorophyll granules to supra-molecular architecture of thylakoid membranes. Photosynth Res 76:185–196

Stiehl HH, Witt HT (1969) Quantitative treatment of the function of plastoquinone in photosynthesis. Z Naturforsch B 24:1588–1598

Stirbet A, Govindjee G (2016) The slow phase of chlorophyll *a* fluorescence induction in silico: origin of the S-M fluorescence rise. Photosynth Res 130:193–213

Stirbet A, Riznichenko GY, Rubin AB, Govindjee G (2014) Modeling chlorophyll *a* fluorescence transient: relation to photosynthesis. Biochemistry (Moscow) 79:291–323

Stirbet A, Lazár D, Guo Y, Govindjee G (2019) Photosynthesis: basics, history, and modeling. Ann Bot. https://doi.org/10.1093/aob/mcz171

Strand DD, Fisher N, Kramer DM (2016) Distinct energetics and regulatory functions of the two major cyclic electron flow pathways in chloroplasts. In: Kirchhoff H (ed) Chloroplasts: current research and future trends. Caister Academic Press, Norfolk, pp 89–100

Suslichenko IS, Tikhonov AN (2019) Photo-reducible plastoquinone pools in chloroplasts of *Tradescentia* plants acclimated to high and low light. FEBS Lett 593:788–798

Tietz S, Puthiyaveetil S, Enlow HM, Yarbrough R, Wood M, Semchonok DA, Lowry T, Li Z, Jahns P, Boekema EJ, Lenhert S, Niyogi KK, Kirchhoff H (2015) Functional implications of Photosystem II crystal formation in photosynthetic membranes. J Biol Chem 290:14091–14106

Tikhonov AN (2012) Energetic and regulatory role of proton potential in chloroplasts. Biochemistry (Moscow) 77:956–974

Tikhonov AN (2013) pH-Dependent regulation of electron transport and ATP synthesis in chloroplasts. Photosynth Res 116:511–534

Tikhonov AN (2014) The cytochrome b_6f complex at the crossroad of photosynthetic electron transport pathways. Plant Physiol Biochem 81:163–183

Tikhonov AN (2015) Induction events and short-term regulation of electron transport in chloroplasts: an overview. Photosynth Res 125:65–94

Tikhonov AN (2016) Modeling electron and proton transport in chloroplasts. In: Kirchhoff H (ed) Chloroplasts: current research and future trends. Caister Academic Press, Norfolk, pp 101–134

Tikhonov AN (2017) Photosynthetic electron and proton transport in chloroplasts: EPR study of ΔpH generation, an overview. Cell Biochem Biophys 75:421–432

Tikhonov AN (2018) The cytochrome b_6f complex: biophysical aspects of its functioning in chloroplasts. In: Harris JR, Boekema EJ (eds) Membrane protein complexes: structure and function, subcellular biochemistry, vol 87. Springer, Singapore, pp 287–328

Tikhonov AN (2020) Structure-function relationships in chloroplasts: EPR study of temperature-dependent regulation of photosynthesis, an overview. In: JR Shen, K Satoh, SI Allakhverdiev (eds) Photosynthesis: molecular approaches to solar energy conversion.

Tikhonov AN, Blumenfeld LA (1985) Hydrogen ions concentration in subcellular systems: physical meaning and the methods for determination. 30:527–537

Tikhonov AN, Subczynski WK (2005) Application of spin labels to membrane bioenergetics (photosynthetic systems of higher plants), chapter 8. In: Eaton SS, Eaton GR, Berliner LJ (eds) Biological magnetic resonance, vol 23. Biomedical EPR—part A: free radicals, metals, medicine, and physiology. Kluwer Academic Publishers, New York, pp 147–194

Tikhonov AN, Vershubskii AV (2014) Computer modeling of electron and proton transport in chloroplasts. BioSystems 121:1–21

Tikhonov AN, Vershubskii AV (2017) Connectivity between electron transport complexes and modulation of photosystem II activity in chloroplasts. Photosynth Res 133:103–114

Tikhonov AN, Khomutov GB, Ruuge EK (1980) Electron spin resonance study of electron transport in photosynthetic systems. IX. Temperature dependence of the kinetics of P700 redox transients in bean chloroplasts induced by flashes with different duration. Mol Biol (Moscow) 14:157–172

Tikhonov AN, Khomutov GB, Ruuge EK, Blumenfeld LA (1981) Electron transport control in chloroplasts. Effects of photosynthetic control monitored by the intrathylakoid pH. Biochem Biophys Acta 637:321–333

Tikhonov AN, Timoshin AA, Blumenfeld LA (1983) Electron transport kinetics, proton transfer, photophosphorylation in chloroplasts, and their relation to thermo-induced structural changes in the thylakoid membrane. Mol Biol (Moscow) 17:1236–1248

Tikhonov AN, Khomutov GB, Ruuge EK (1984) Electron transport control in chloroplasts. Effects of magnesium ions on the electron flow between two photosystems. Photobiochem Photobiophys 8:261–269

Tikhonov AN, Agafonov RV, Grigor'ev IA, Kirilyuk IA, Ptushenko VV, Trubitsin BV (2008) Spin-probes designed for measuring the intrathylakoid pH in chloroplasts. Biochim BiophysActa 1777:285–294

Timoshin AA, Tikhonov AN, Blumenfeld LA (1984) Thermoinduced structural changes in ATP-synthase as a factor of energy transduction control in chloroplasts. Biophysics 29:338–340

Torres-Pereira J, Mehlhorn R, Keith AD, Packer L (1974) Changes in membrane lipid structure of illuminated chloroplasts—studies with spin labeled and freeze-fractured membranes. Arch Biochem Biophys 160:90–99

Tremmel IG, Kirchhoff H, Weis E, Farquhar GD (2003) Dependence of plastoquinol diffusion on the shape, size, and density of integral thylakoid proteins. Biochim Biophys Acta 1603:97–109

Trubitsin BV, Tikhonov AN (2003) Determination of a transmembrane pH difference in chloroplasts with a spin label tempamine. J Magn Reson 163:257–269

Turina P, Petersen J, Gräber P (2016) Thermodynamics of proton transport coupled ATP synthesis. Biochim Biophys Acta 1857:653–664

Ustynyuk LYu, Tikhonov AN (2018) The cytochrome b_6f complex: DFT modeling of the first step of plastoquinol oxidation by the iron-sulfur protein. J Organomet Chem 867:290–299

Varco-Merth B, Fromme R, Wang M, Fromme P (2008) Crystallization of the c_{14}-rotor of the chloroplast ATP synthase reveals that it contains pigments. Biochim Biophys Acta 1777:605–612

Vershubskii AV, Tikhonov AN (2020) pH-Dependent regulation of electron and proton transport in chloroplasts in situ and in silico. Biochem (Moscow) Suppl Ser A 14:154–165

Vershubskii AV, Kuvykin IV, Priklonsky VI, Tikhonov AN (2011) Functional and topological aspects of pH-dependent regulation of electron and proton transport in chloroplasts in silico. Biosystems 103:164–179

Vershubskii AV, Trubitsin BV, Priklonskii VI, Tikhonov AN (2017) Lateral heterogeneity of the proton potential along the thylakoid membranes of chloroplasts. Biochim Biophys Acta 1859:388–401

Vershubskii AV, Nevyantsev SM, Tikhonov AN (2018) Modeling of electron and proton transport in chloroplast membranes with regard to thioredoxin-dependent activation of the Calvin-Benson cycle and ATP synthase. Biochem(Moscow) Suppl Ser A 12:287–302

Vlasov AV, Kovalev KV, Marx S-H et al (2019) Unusual features of the c-ring of F_1F_O ATP synthases. Sci Rep 9(1):1–11

Vollmar M, Schlieper D, Winn M, Büchner C, Groth G (2009) Structure of the c_{14} rotor ring of the proton translocating chloroplast ATP synthase. J Biol Chem 284:18228–18235

Wada H, Murata N (eds) (2009) Lipids in Photosynthesis: Essential and Regulatory Functions. Springer, Dordrecht

Walker JE (2013) The ATP synthase: the understood, the uncertain and the unknown. Biochem Soc Trans 41:1–16

Wallis JG, Browse J (2002) Mutants of *Arabidopsis* reveal many roles for membrane lipids. Prog Lipid Res 41:254–278

Witt HT (1979) Energy conversion in the functional membrane of photosynthesis. Analysis by light pulse and electric pulse methods. Biochim Biophys Acta 505:355–427

Yamamoto Y (2016) Quality control of photosystem II: the mechanisms for avoidance and tolerance of light and heat stresses are closely linked to membrane fluidity of the thylakoids. Front Plant Sci 7:1136. https://doi.org/10.3389/fpls.2016.01136

Yamamoto Y, Nishimura M (1976) Characteristics of light-induced H^+ transport in spinach chloroplasts at lower temperatures I. Relationship between H^+ transport and physical changes of the microenvironment in chloroplast membranes. Plant Cell Physiol 17:11–16

Yamamoto Y, Ford RC, Barber J (1981) Relationship between thylakoid membrane fluidity and the functioning of pea chloroplasts. Effect of cholesteryl hemisuccinate. Plant Physiol 67:1069–1072

Yamori W, Hikosaka K, Way DA (2014) Temperature response of photosynthesis in C3, C4, and CAM plants: temperature acclimation ant temperature adaptation. Photosynth Res 119:101–117

Yan J, Cramer WA (2003) Functional insensitivity of the cytochrome b_6f complex to structure changes in the hinge region of the Rieske iron–sulfur protein. J Biol Chem 278:20926–20933

Yan K, Chen P, Shao H, Shao C, Zhao S, Brestic M (2013) Dissection of photosynthetic electron transport process in sweet sorghum under heat stress. PLoS ONE 8(5):e62100

Zaks J, Amarnath K, Kramer DM, Niyogi KK, Fleming GR (2012) A kinetic model of rapidly reversible nonphotochemical quenching. Proc Natl Acad Sci USA 109:15757–15762

Zhou Y, vom Dorp K, Dörman P, Hölzl G (2016) Chloroplast lipids. In: Kirchhoff H (ed) Chloroplasts: current research and future trends. Caister Academic Press, Norfolk, pp 1–24

Zhu XG, Wang Y, Ort DR, Long SP (2013) e-Photosynthesis: a comprehensive dynamic mechanistic model of C3 photosynthesis: from light capture to sucrose synthesis. Plant Cell Environ 36:1711–1727